

UNCLASSIFIED

AD 401 139

*Reproduced
by the*

DEFENSE DOCUMENTATION CENTER

FOR

SCIENTIFIC AND TECHNICAL INFORMATION

CAMERON STATION, ALEXANDRIA, VIRGINIA



UNCLASSIFIED

NOTICE: When government or other drawings, specifications or other data are used for any purpose other than in connection with a definitely related government procurement operation, the U. S. Government thereby incurs no responsibility, nor any obligation whatsoever; and the fact that the Government may have formulated, furnished, or in any way supplied the said drawings, specifications, or other data is not to be regarded by implication or otherwise as in any manner licensing the holder or any other person or corporation, or conveying any rights or permission to manufacture, use or sell any patented invention that may in any way be related thereto.

63-3-2

CATALOGED BY ASTIA
AS AD NO. 401139

Test Time in Low Pressure Shock Tubes

27 DECEMBER 1962

Prepared by HAROLD MIRELS
Aerodynamics and Propulsion Research Laboratory

Prepared for COMMANDER SPACE SYSTEMS DIVISION

UNITED STATES AIR FORCE

Inglewood, California

401139

APR 10 1963

ASTIA



LABORATORIES DIVISION • AEROSPACE CORPORATION

CONTRACT NO. AF 04(695)-169

TEST TIME IN LOW PRESSURE SHOCK TUBES

Prepared by
Harold Mirels
Aerodynamics and Propulsion Research Laboratory

AEROSPACE CORPORATION
El Segundo, California

Contract No. AF 04(695)-169

27 December 1962

Prepared for
COMMANDER SPACE SYSTEMS DIVISION
UNITED STATES AIR FORCE
Inglewood, California

ABSTRACT

The reduction of test time in low pressure shock tubes, due to a laminar wall boundary layer, has been analytically investigated. In previous studies by Roshko and Hooker the flow was considered in a contact surface fixed co-ordinate system. In the present study it was assumed that the shock moves with uniform velocity, and the flow was investigated in a shock fixed co-ordinate system. Unlike the previous studies, the variation of free stream conditions between the shock and contact surface was taken into account. It was found that β , a parameter defined by Roshko, is considerably larger than the estimates made by Roshko and Hooker except for very strong shocks. Since test time is proportional to β^{-2} , previous estimates of test time are too large, particularly for weak shocks. The present estimates for β appear to agree with existing experimental data to within about 10 percent for shock Mach numbers greater than 5. In other respects, the basic theory is in general agreement with the previous results of Roshko.

CONTENTS

I.	INTRODUCTION	1
II.	STEADY STATE SOLUTION	5
	A. UNIFORM EXTERNAL FREE STREAM APPROXIMATION	8
	B. LOCAL SIMILARITY APPROXIMATION	11
	C. SUMMARY AND DISCUSSION OF RESULTS	22
III.	UNSTEADY SOLUTION	31
	A. SEPARATION BETWEEN SHOCK AND CONTACT SURFACE	31
	B. TEST TIME	36
IV.	COMPARISON WITH REFERENCES 8 AND 10	41
V.	COMPARISON WITH EXPERIMENTAL DATA	47
VI.	ADDITIONAL CONSIDERATIONS	51
	A. FLOW NONUNIFORMITY	51
	B. COMPARISON OF IDEAL AND ACTUAL ASYMPTOTIC SHOCK STRENGTH	51
	C. TRANSITION	53
	D. BOUNDARY LAYER THICKNESS AT l_m	55
VII.	SUMMARY AND CONCLUDING REMARKS	59
	APPENDIX. BOUNDARY LAYER BEHIND MOVING SHOCK	61
	REFERENCES	69

TABLES

1	Evaluation of β_0 , β_1 , and β_2 Assuming Ideal Gas and Boundary Layer With $\rho\mu = \text{constant}$	24
2	Values of β For Air Using Real Gas Boundary Layer Solution of Reference 13	26
3	Evaluation of β From Experimental Data in Fig. 14	49
A-1	Parameters Defining Boundary Layer Behind Shock Moving with Uniform Velocity, Assuming an Ideal Gas and $\rho\mu = \text{Constant}$	64

FIGURES

1	Shock Tube Flow in Laboratory Coordinates	2
2	Flow between Shock and Contact Surface in Shock-Stationary Coordinate System	6
3	Boundary Layer Development Assuming Uniform Free Stream	9
4	Boundary Layer Development with Uniform Free Stream, Wall Velocity u_w , and Origin at l_1	13
5	Variation of Boundary Layer Excess Mass Flow, $\bar{\delta}$, With ξ	15
6	Values of β for Ideal Gas With Constant γ , σ , and $\rho\mu$	25
7	Values of β For Air (Based on Equilibrium Real Gas Properties, $p_{\infty} \approx 0.001$ atm) and for Argon, Including Effect of Variable $\rho\mu$	27
8	Separation Distance for Air and Argon Including Effect of Variable $\rho\mu$	29
9	Flow Model for Finding Separation Distance Between Shock and Contact Surface as a Function of Time	33
10	Variation of T With X From Numerical Integration of Eq. (32) (For Ideal Gas, $\sigma = 1$ and $\rho\mu = \text{Constant}$) and From Eq. (35)	35
11	Determination of Test Time at x_a	38
12	Test Time at Given Station	39
13	Flow in Contact Surface Fixed Coordinate System of References 8 and 10	42
14	Experimental Results of References 7, 8, and 10, Reduced on the Basis of $\beta = \sqrt{3}$ and $T = \bar{T}$ (Modified from Fig. 3, Ref. 10)	48
15	Reynolds Number at Contact Surface (Eq. 53)	56
16	Boundary Layer Thickness at l_m Corresponding to $(u_w - u)/(u_w - u_{e,o}) = 0.99$	58

I. INTRODUCTION

In an ideal shock tube (i. e. , neglecting wall and real gas effects), the shock and the contact surface both move with a constant velocity and the flow between them is uniform (Fig. 1). In an actual shock tube flow, however, the presence of a wall boundary layer causes the shock to decelerate, the contact surface to accelerate, and the flow to be nonuniform (e. g. , Ref. 1). Analytical and experimental studies of the nonuniformities in shock tube flows have been presented in References 1 through 10 (as well as by others).

The analytical theory presented in References 5 and 6 is applicable when the wall boundary layer introduces only small perturbations into the ideal flow. In these references, it was shown that the wall boundary layer between the shock and the contact surface acts as an aerodynamic sink, removing mass from the region between the shock and the contact surface. This mass removal causes the shock to decelerate and the contact surface to accelerate, in agreement with the experimental observations of Reference 1.

As the length-to-diameter ratio of a shock tube is increased and as the initial pressure in the low pressure section is reduced, the wall boundary layer effects become more pronounced. (The study of dissociation and ionization in shock tubes has stimulated the use of low initial pressures.) Duff,⁷ in a study of the flow about 12 feet from the diaphragm in a 1-1/8 in. diameter shock tube with initial pressures of the order of 1 mm Hg, found the flow to be strikingly different from that in a conventional shock tube. In a conventional tube, the separation between the shock and the contact surface (and therefore the test time) increases with distance from the diaphragm. However, in a low pressure shock tube, Duff observed that the separation reaches a limiting value and remains constant with distance thereafter. When this limiting condition is reached, the shock and the contact surface both move with equal and constant velocity. This phenomenon must be taken into account when estimating test time in low density shock tubes.

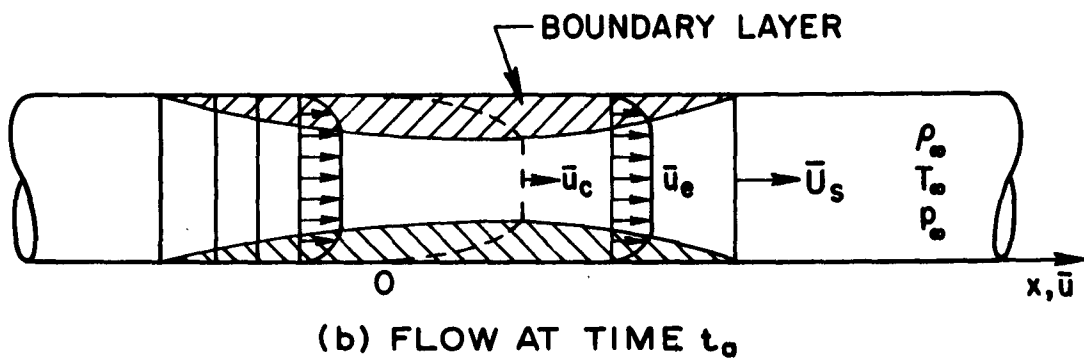
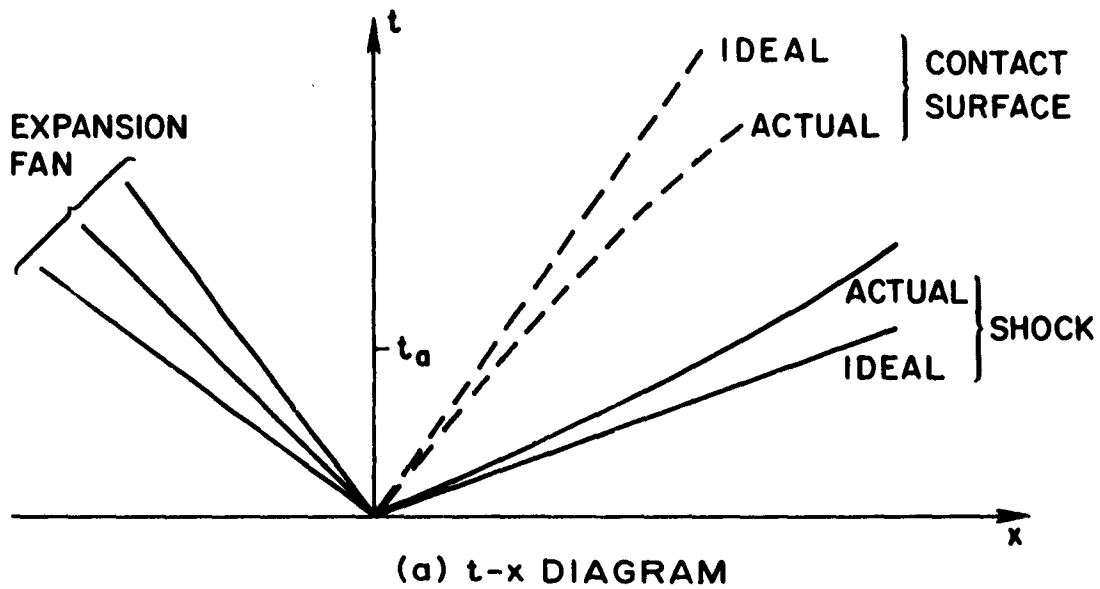


Fig. 1. Shock Tube Flow in Laboratory Coordinates

Duff correctly explained the limiting flow, where shock and contact surface move with equal velocity, as one wherein the flow passing through the shock equals the flow which moves past the contact surface due to the wall boundary layer. He referred to the contact surface as a "leaky piston." This effect was later studied experimentally and analytically by Roshko.⁸ In the analytical portion of Reference 8, Roshko considered the flow in a co-ordinate system in which the contact surface was stationary. The separation distance between the shock and contact surface at any instant was found from a mass balance that equated the mass flow through the shock to the sum of the boundary layer mass flow moving past the contact surface and the rate of accumulation of mass between the shock and contact surface. (Anderson⁹ had used a similar approach.) Roshko used the boundary layer theory presented in References 11 and 12 (which applies for the boundary layer behind a shock moving with uniform velocity). He also developed an approximate boundary layer theory to account for real gas effects. (The latter are treated more accurately in Refs. 13 and 16.) Experimental measurements of test time for a variety of initial pressures were obtained by Roshko, which confirmed the basic theory.

Hooker¹⁰ noted an erroneous velocity transformation in Reference 8 and also noted that Roshko had left out a term in the mass balance equation, namely, the accumulation of mass between the shock and contact surface due to nonuniform density in the boundary layer. He proceeded to correct Roshko's theory for these effects and claimed a somewhat improved correlation between theory and experiment. However, the improvement was not dramatic.

The analytical results of Roshko and Hooker describe the basic features of the flow in a low density shock tube and are widely used to estimate test time. However, the flow model used in both papers (i. e. , a co-ordinate system in which the contact surface is fixed) contains several inherent contradictions. For example, both authors solve for the nonuniform shock velocity relative to the contact surface but assume, for one term in the mass balance equation, that the shock velocity is constant. The nonuniformity of the flow between the shock and the contact surface is not taken into account since both authors use a boundary

layer theory based on uniform flow between the shock and the contact surface. They recognized that the latter assumption becomes correct only in the case of very strong shocks but made no attempt to modify the theory for the "not-so-strong" shock despite the fact that much of their experimental data were obtained at moderate Mach numbers.

In the present paper, the problem of test time in a low density shock tube is investigated by considering a flow model wherein the shock moves with uniform velocity. The co-ordinate system is one in which the shock is stationary, and the wall moves. The present model is self-consistent. A boundary layer theory is developed to take into account the nonuniform flow between the shock and the contact surface. The solution applies to shocks of moderate strength, as well as to strong shocks. Previous experimental data are re-examined in the light of the present theory.

II. STEADY STATE SOLUTION

The experimental results presented in References 7, 8, and 10 indicate that the shocked gas in a low density shock tube ultimately reaches a steady state condition where both the shock and the contact surface move with equal and constant velocity. The flow between the shock and the contact surface is then steady when viewed in a co-ordinate system in which the shock and the contact surface are stationary. In this co-ordinate system the wall moves with velocity u_w (which equals the shock velocity U_s in the laboratory system). This steady flow is investigated herein with the primary object of determining the separation distance between the shock and the contact surface. The problem of unsteady flow, where the shock and the contact surface have different velocities, is treated in Section III.

Steady flow is illustrated in Fig. 2. The shock is located at $l = 0$, and the free stream portion of the contact surface at $l = l_m$. The flow upstream of the shock is denoted by subscript ∞ and moves with velocity u_w , as does the wall. Free stream conditions between the shock and the contact surface are denoted by subscript e . Free stream conditions directly downstream of the shock have the additional subscript o . The percentage of mass flow in the boundary layer increases with l such that all the mass flow is in the boundary layer at l_m and the free stream is stationary at that location.

Roshko⁸ obtained an estimate for l_m in the following manner. The flow rate through the shock, \dot{m}_s , equals

$$\dot{m}_s = (\rho_e u_e)_o A \quad (1a)$$

where A is the cross-sectional area of the tube. Roshko assumed that the boundary layer was thin and characterized the flow in the boundary layer at the contact surface, \dot{m}_c , by

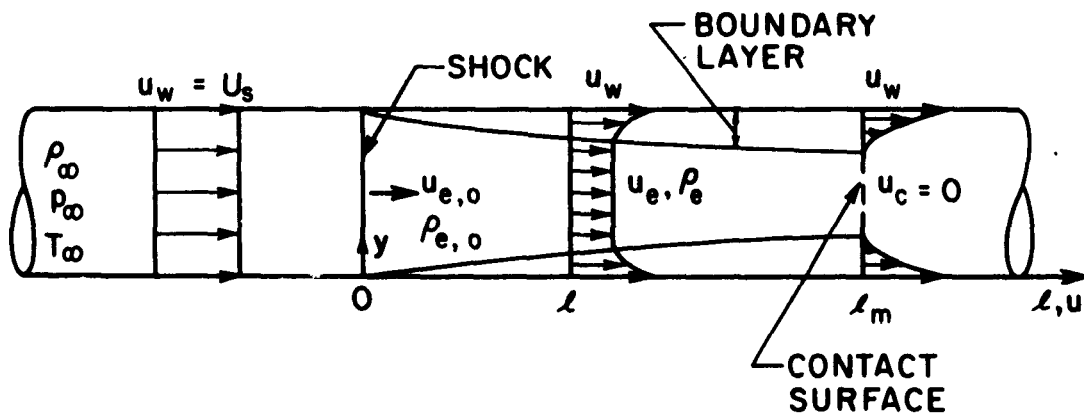


Fig. 2. Flow Between Shock and Contact Surface
In Shock-Stationary Coordinate System

$$\dot{m}_c = L\rho_{w,o}(u_w - u_{e,o})\delta_R \quad (1b)$$

where L is the perimeter of the tube; δ_R is a characteristic boundary layer thickness at l_m ; and $\rho_{w,o}$ and $u_w - u_{e,o}$ are characteristic boundary layer densities and velocities, respectively. The boundary layer thickness was further characterized by

$$\delta_R \equiv \beta \sqrt{\frac{v_{w,o} l_m}{u_w - u_{e,o}}} \quad (1c)$$

where β is a constant that must be found from an exact solution of the boundary layer development in the tube. Equating Eqs. (1a) and (1b), since the flow is steady, yields the following expression for l_m :

$$l_m = \frac{d^2}{16\beta^2} \left(\frac{\rho_{e,o}}{\rho_{w,o}} \right)^2 \frac{u_{e,o}}{u_w - u_{e,o}} \frac{u_{e,o}}{v_{w,o}} \quad (2)$$

where $d \equiv 4A/L$ is the hydraulic diameter. Assume that the temperature upstream of the shock is at a standard condition so that $T_\infty = T_{st}$, $a_\infty = a_{st}$, and $\mu_\infty = \mu_{st}$. Also, assume that the wall remains at its initial temperature so that $T_w = T_{st}$. From continuity, $\rho_\infty u_w = (\rho_e u_e)_o$. Equation (2) can then be put in the form

$$\frac{p_{st}}{p_\infty} \frac{l_m}{d^2} = \frac{1}{16\beta^2} \frac{p_\infty}{p_{e,o}} \frac{WM_s}{W-1} \left(\frac{\rho a}{\mu} \right)_{st} \quad (3)$$

where $W \equiv u_w/u_{e,o} \equiv \rho_{e,o}/\rho_\infty$, $M_s \equiv u_w/a_\infty$, and p_{st} is a standard pressure (usually an atmosphere). The right hand side of Eq. (3) depends primarily on M_s . Hence, for a given M_s , the separation distance l_m is proportional

to the product $d^2 p_\infty$. This can result in very short test times for shock tubes with low initial pressure.

Equation (3) does not yield numerical results for l_m unless an accurate estimate of β is available. Estimates of β have been presented in References 8, 10, and 14. The primary purpose of the present paper is to improve these estimates, particularly for flows with moderate M_s . This is done by taking Eq. (2) as the defining relation for β

$$\beta^2 \equiv \frac{d^2}{16l_m} \left(\frac{\rho_{e,o}}{\rho_{w,o}} \right)^2 \frac{1}{W-1} \frac{u_{e,o}}{v_{w,o}} \quad (4)$$

and finding l_m as accurately as possible from a consideration of the boundary layer development in the flow illustrated in Fig. 2. A first estimate is made below by considering the boundary layer to develop in a uniform external stream. An improved estimate is then made by employing the concept of local similarity.

A. UNIFORM EXTERNAL FREE STREAM APPROXIMATION

Boundary layer development for the case of an external free stream that does not vary with l is illustrated in Fig. 3 and is discussed in the Appendix. Let l_m correspond to the value of l at which the excess mass flow in the boundary layer equals the mass flow entering through the shock. This gives

$A(\rho_e u_e)_o = L(\rho_e u_e)_o (-\delta^*)$ where δ^* is the boundary layer displacement thickness at l_m . Combining the latter expression with Eqs. (4) and (A-4) (Appendix) yields

$$\beta_o = \sqrt{\frac{2}{W-1}} [(f - \eta)_\infty + I_\infty]_o \equiv \sqrt{\frac{2}{W-1}} G_o \quad (5a)$$

The subscript o has been added to β to indicate that this value is based on a boundary layer with a uniform external stream.

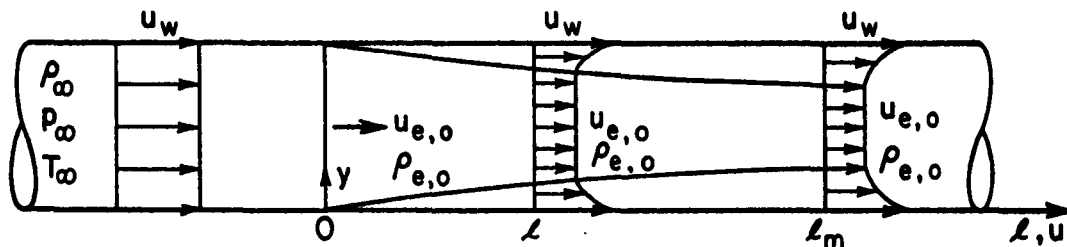


Fig. 3. Boundary Layer Development Assuming Uniform Free Stream

Numerical values of β_o have been computed assuming an ideal gas and $\rho\mu = \text{constant}$ in the boundary layer (Appendix). These are listed in Table 1 for Prandtl number (σ) = 0.72 and 1; $\gamma = 7/5$ and $5/3$; and for various shock strengths.

A solution for the boundary layer behind a strong shock moving with uniform velocity into air at an initial pressure of 0.001 atmospheres and $T_w = T_\infty = 522^\circ\text{R}$ has been presented in Reference 13. (Some results at 0.01 atmospheres were also obtained.) This is a "real gas" solution in the sense that equilibrium gas charts were used to obtain the flow across the shock and in the boundary layer. The Sutherland relationship was used to evaluate the variation of $\rho\mu$ in the boundary layer. Some of the boundary layer results are given in Table 2. The corresponding values of β_o are included in this Table.

It is expected that these values of β_o will overestimate l_m particularly for shock Mach numbers that are not large. This is due to the fact that the relative velocity between the wall and the free stream increases from $u_w - u_{e,o}$ at $l = 0$ to u_w at l_m (compare Figs. 2 and 3). Hence the excess mass flow in the boundary layer will be greater at a given l than that obtained from the above model (which assumes the relative velocity to remain constant at $u_w - u_{e,o}$). This will result in smaller l_m and larger β than obtained from Eq. (5a). However, for very strong shocks, where $u_{e,o}$ is small relative to u_w , Eq. (5a) should give accurate results.

In Reference 8, Roshko used two different expressions to evaluate β . The first expression arose from a velocity transformation error (pointed out by Hooker) and is the same as Eq. (5a). His results for $\sigma = 1$, $\gamma = 7/5$ (in Table I of Ref. 8) are in agreement with Table 1 herein. He also used the expression

$$\beta_R \equiv \sqrt{\frac{2}{W-1}} [(l - \eta)_\infty]_o \quad (5b)$$

which is the basis for the results he presents in his Tables II to IV. Since $I_{\infty}/(f - \eta)_{\infty}$ is positive, β_R is somewhat smaller than β_0 and therefore leads to greater error when computing l_m . Equation (5b) is the expression that arises naturally from the contact surface fixed co-ordinate system used in Reference 8 and is presumably the expression Roshko meant to employ throughout his paper. In References 10 and 14, Eq. (5b) was therefore used to evaluate β . This is discussed further in Section IV.

B. LOCAL SIMILARITY APPROXIMATION

In the present section, the streamwise variation of free stream properties due to the increase in boundary layer mass flow with l is taken into account. The development of the boundary layer and the variation in free stream properties are treated simultaneously. The boundary layer growth is found by assuming that at each station it is similar to a corresponding boundary layer developing in a uniform free stream behind a shock moving with uniform velocity (i. e., local similarity).

Since the flow is steady (Fig. 2), the net mass flow through the shock equals the net mass flow at any station l . Thus

$$A(\rho_e u_e)_0 = A\rho_e u_e + L \int_0^{\infty} (\rho u - \rho_e u_e) dy \quad (6)$$

In Eq. (6), it is assumed that the boundary layer thickness is small compared with d ; thus the integrand is nonzero only in the region close to the wall.

Define

$$\bar{\delta} \equiv \frac{4}{d} \frac{\rho_e u_e}{(\rho_e u_e)_0} (-\delta^*) \quad (7a)$$

where δ^* is the local boundary layer thickness

$$\delta^* = \int_0^{\infty} \left(1 - \frac{\rho u}{\rho_e u_e} \right) dy \quad (7b)$$

Note that $\bar{\delta}$ is the ratio of the excess mass flow through the boundary layer at l , to the mass flow through the shock. Thus $\bar{\delta}$ varies from 0 at $l = 0$ to 1 at $l = l_m$. Equations (6) and (7) then give

$$\bar{\delta} = 1 - \frac{\rho_e u_e}{(\rho_e u_e)_o} \quad (8)$$

which relates the free stream conditions to the local boundary layer displacement thickness.

The concept of local similarity is now introduced. It is assumed that the boundary layer profile at each l corresponds to that for a boundary layer associated with a uniform free stream (equal to the local free stream) and a wall velocity u_w . The origin of this boundary layer is at l_i , which is initially an unknown function of l . (See Fig. 4.) The origin l_i is chosen such that the excess flow in the boundary layer at each l has the correct local value. It is also assumed that the boundary layer growth at each section is the same as that for the corresponding uniform free stream boundary layer.

The local displacement thickness is then (Eq. A-4)

$$-\delta^* = \frac{\rho_w}{\rho_e} \sqrt{\frac{2(l - l_i) v_w}{u_e}} [(f - \eta)_{\infty} + I_{\infty}] \quad (9)$$

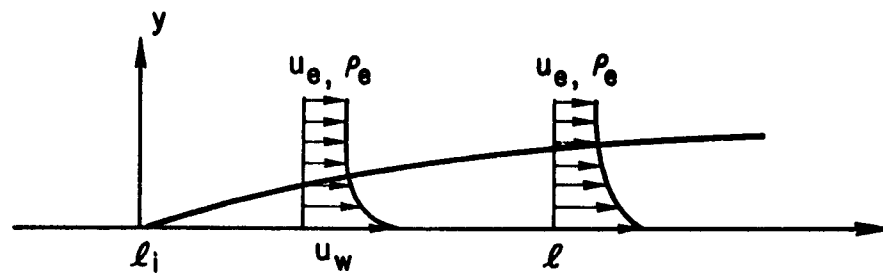


Fig. 4. Boundary Layer Development With Uniform Free Stream, Wall Velocity u_w , and Origin at l_i

where $(f - \eta)_{\infty}$ and I_{∞} are functions of the local free stream and wall conditions (Appendix). From Eq. (7a), $\bar{\delta}$ becomes

$$\bar{\delta} = \sqrt{\xi - \xi_1} H_e \quad (10a)$$

where

$$\xi \equiv 2 \left[\frac{4}{d} \left(\frac{\rho_w}{\rho_e} \right) \right]^2 \frac{v_{w,o}}{u_{e,o}} l \quad (10b)$$

$$\xi_1 \equiv 2 \left[\frac{4}{d} \left(\frac{\rho_w}{\rho_e} \right) \right]^2 \frac{v_{w,o}}{u_{e,o}} l_i \quad (10c)$$

$$H_e = \sqrt{V \frac{P_e}{P_{e,o}}} [(f - \eta)_{\infty} + I_{\infty}] \quad (10d)$$

$$V \equiv u_e / u_{e,o} \quad (10e)$$

The nondimensional variable ξ now replaces l . In deriving Eq. (10a) from Eqs. (7a) and (9), it was assumed that $T_w = T_{w,o}$ and $\mu_w = \mu_{w,o}$.

The problem now is to solve Eqs. (8) and (10a) simultaneously to find $\bar{\delta}$ as a function of ξ . The value of ξ at $\bar{\delta} = 1$ will then define l_m and β . First, ξ_1 will be eliminated. Since $\bar{\delta}$ is a function of ξ , a plot of $\bar{\delta}$ versus ξ can be made, as indicated by the solid line in Fig. 5. The dashed line in Fig. 5 represents the variation of $\bar{\delta}$ with ξ for a boundary layer growing under a uniform free stream corresponding to the free stream condition H_e at some station ξ . The origin of this boundary layer, ξ_1 , is such that $\bar{\delta}$ has the correct value at ξ . The boundary layer is assumed to grow at ξ at the same

- ACTUAL VARIATION OF $\bar{\delta}$ WITH ξ .
- - - VARIATION OF $\bar{\delta}$ WITH ξ FOR BOUNDARY LAYER WITH ORIGIN AT ξ_i AND FREE STREAM H_e .
- · - · VARIATION OF $\bar{\delta}$ WITH ξ FOR BOUNDARY LAYER WITH ORIGIN AT $\xi_i + \Delta\xi_i$ AND FREE STREAM $H_e + \Delta H_e$.

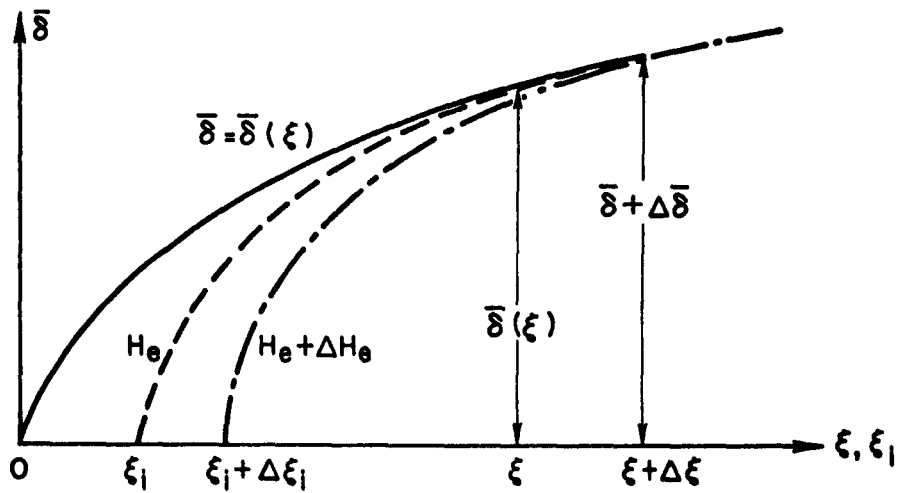


Fig. 5. Variation of Boundary Layer Excess Mass Flow, $\bar{\delta}$, With ξ

rate as the corresponding uniform free stream boundary layer (dashed line). The value of $\bar{\delta}$ at some point $\xi + \Delta\xi$ is then

$$\bar{\delta} + \Delta\bar{\delta} = \sqrt{(\xi + \Delta\xi) - \xi_i} H_e \quad (11)$$

However, the boundary layer at $\xi + \Delta\xi$ may be viewed as corresponding to a boundary layer originating at $\xi_i + \Delta\xi_i$ and developing under a uniform free stream corresponding to the free stream at $\xi + \Delta\xi$. The latter free stream is characterized by the value $H_e + \Delta H_e$. The resulting boundary layer is denoted by the dash-dot curve in Fig. 5. The choice of $\Delta\xi_i$ is such that the excess mass flow in the boundary layer $\bar{\delta} + \Delta\bar{\delta}$ at $\xi + \Delta\xi$ is the same as for the boundary layer originating at ξ_i . Thus

$$\bar{\delta} + \Delta\bar{\delta} = \sqrt{(\xi + \Delta\xi) - (\xi_i + \Delta\xi_i)} (H_e + \Delta H_e). \quad (12)$$

Equating Eqs. (11) and (12) and neglecting higher order terms gives

$$\frac{1}{2} \frac{\Delta\xi_i}{\xi - \xi_i} = \frac{\Delta H_e}{H_e} \quad (13)$$

which relates $\Delta\xi_i$ and ΔH_e .

The total differential of Eq. (10a) is

$$\frac{\Delta\bar{\delta}}{\bar{\delta}} = \frac{1}{2} \frac{\Delta\xi - \Delta\xi_i}{\xi - \xi_i} + \frac{\Delta H_e}{H_e} \quad (14)$$

In view of Eq. (13) this becomes

$$\frac{\Delta\bar{\delta}}{\bar{\delta}} = \frac{1}{2} \frac{\Delta\xi}{\xi - \xi_i} \quad (15)$$

But, from Eq. (10a), $\xi - \xi_i = \bar{\delta}^2/H_e^2$. Hence, Eq. (15) becomes $\bar{\delta}\Delta\bar{\delta}/H_e^2 = \Delta\xi/2$, or in integral form

$$\xi = 2 \int_0^{\bar{\delta}} \frac{\bar{\delta} d\bar{\delta}}{H_e^2} \quad (16)$$

This expression can be integrated to find ξ as a function of $\bar{\delta}$. The value of ξ at $\bar{\delta} = 1$ is denoted ξ_m and defines l_m . In particular, from Eqs. (4) and (10b),

$$\beta = \sqrt{\frac{2}{(W-1)\xi_m}} \equiv \beta_2 \text{ or } \beta_1 \quad (17)$$

The subscript 2 is used when ξ_m is obtained from a numerical integration of Eq. (16). The subscript 1 is used when ξ_m is obtained from an approximate integration, as will be discussed later.

In order to integrate Eq. (16) it is necessary to express H_e as a function of $\bar{\delta}$. A procedure for doing this is outlined by Eqs. (A-13) through (A-16) in the Appendix. These equations apply for an ideal gas where $\sigma = 1$ and $\rho\mu = \text{constant}$ across the boundary layer. A numerical integration of Eq. (16) is required. This has been done for $\gamma = 7/5$, $\gamma = 5/3$, and values of W from 1.100 through 6. The results for β_2 are included in Table 1. These will be discussed later.

Approximate Analytical Integration of Eq. (16)

Equation (16) requires a numerical integration and only the case of an ideal gas where $\sigma = 1$ and $\rho\mu = \text{constant}$ has been evaluated. In the present section, an approximate analytical integration of Eq. (16) is obtained which is suggested by the solution for strong shocks. It will be shown that this approximate integration gives accurate results for all M_s , except M_s near 1.

For $M_{e,o}^2 \ll 1$ (i. e., for strong shocks), the state properties of the fluid in the free stream between $\xi = 0$ and $\xi = \xi_m$ can be assumed to remain constant. That is, $[\rho_e/\rho_{e,o}]^{\gamma} = p_e/p_{e,o} \approx 1 + 0(M_{e,o})^2$. Equations (8) and (10d) become

$$\bar{\delta} = 1 - V \quad (18a)$$

$$H_e = \sqrt{V} [(f - \eta)_{\infty} + I_{\infty}] \quad (18b)$$

We now assume that $1 + I_{\infty}/(f - \eta)_{\infty}$ remains fairly constant for a given flow and may be taken equal to its value at $\xi = 0$. (Note from Tables 2 and A-1 that $I_{\infty}/(f - \eta)_{\infty}$ is small for strong shocks. However, $I_{\infty}/(f - \eta)_{\infty}$ decreases with V (Eq. A-12) so that the present approximation tends to overestimate G .) Equation (18b) now becomes

$$H_e = \sqrt{V} \frac{(f - \eta)_{\infty}}{[(f - \eta)_{\infty}]_0} G_o \quad (19a)$$

$$= \frac{W - V}{W - 1} \frac{\sqrt{1 + 1.022W}}{\sqrt{V + 1.022W}} G_o \quad (19b)$$

where the substitution for $\sqrt{V} (f - \eta)_{\infty}/(f - \eta)_{\infty,0}$ in going from Eq. (19a) to Eq. (19b) was found from Eqs. (A-8a) and (A-10a). In effect, Eq. (19b) assumes that the change in H_e is due primarily to changes in boundary layer velocity profile. Substitution of Eqs. (18a) and (19b) into Eq. (16) yields

$$\xi = \frac{1}{B} \int_V^1 \frac{(1 - V)(1 + DV)dV}{(1 - EV)^2} \quad (20a)$$

where

$$B = \frac{W}{2.044} \frac{1 + 1.022 W}{(W - 1)^2} G_o^2 \quad (20b)$$

$$D = 1/1.022 W \quad (20c)$$

$$E = 1/W \quad (20d)$$

Equation (20a) can be integrated and gives, for $V = 0$,

$$\xi_m = \frac{1}{BE^2} \left[\frac{DE - E - 2D}{E} \ln(1 - E) - E - 2D \right] \quad (21a)$$

$$\approx \frac{3 + D + 2E}{6B} [1 + o(1/W^2)] \quad (21b)$$

These equations become, in terms of W and G_o ,

$$\xi_m = \frac{6.044}{G_o^2} \frac{(W - 1)^2}{1 + 1.022 W} \left[\left(W - \frac{1}{3.022} \right) \ln \left(\frac{W}{W - 1} \right) - 1 \right] \quad (22a)$$

$$\approx \frac{1}{G_o^2} \left[\frac{W - 1}{W} \right]^2 [1 + o(1/W^2)] \quad (22b)$$

In deriving Eq. (22b), a term $0.015/W$ was neglected compared with 1.

Equations (22) can be used, with Eq. (17), to find β . The resulting values of β are given the subscript 1 to indicate that they are obtained from the approximate integration of Eq. (16). Values of β_1 obtained from Eqs. (22), are included in Tables 1 and 2 and will also be discussed later.

The parameter β_1 has a simple relation to β_0 when $W^2 \gg 1$. Thus, from Eqs. (5), (17), and (22b)

$$\beta_1 = \beta_0 \frac{W}{W-1} [1 + 0(1/W^2)] \quad (23)$$

It is seen that β_1 is larger than β_0 but approaches β_0 as $W \rightarrow \infty$.

Simplified Expressions for β_1

Equations (17) and (22) indicate that β_1 depends only on W and G_0 . The value of W is found from normal shock relations and can be considered known. The problem then is to find G_0 . In References 12 and 13, analytic interpolation formulas for G_0 have been presented. These are used herein to obtain simple analytic expressions for β_1 .

For an ideal gas with $\rho\mu$ constant in the boundary layer

$$G_0 = \frac{1.135(W-1)}{\sqrt{1+1.022W}} \left[1 + \frac{I_\infty}{(f-\eta)_{\infty 0}} \right]_0 \quad (24)$$

where the coefficient of the bracketed term is $(f-\eta)_{\infty 0}$ (see Eq. A-8a). Substituting into Eqs. (17) and (22b) and neglecting a term $0.01/W$ compared with 1 yields

$$\beta_1 = 1.59 \left[1 + \frac{I_\infty}{(f-\eta)_{\infty 0}} \right]_0 [1 + 0(1/W^2)] \quad (25)$$

The ratio $\left[\frac{I_\infty}{(f-\eta)_{\infty 0}} \right]_0$ has been evaluated for $\sigma = 1$ in the Appendix. Substituting Eq. (A-9b) into Eq. (25) gives

$$\beta_1 = 1.59 \left[1 + \frac{0.562W}{ZW-1} \left(1 + \frac{2.57}{W} \right) \right] [1 + 0(1/W^2)] \quad (26a)$$

This agrees with the values of β_1 in Table 1 for $\sigma = 1$ and $\gamma = 7/5$ and $5/3$ to within 3 percent for $W \geq 2$. A similar expression can be derived to correlate the $\sigma = 0.72$ data in Table 1. If the constants in the expression for $[I_\infty / (f - \eta)_{\infty}]_0$ are adjusted so that β_1 has the correct value at $W = 6$, $\gamma = 7/5$ and $W = 4$, $\gamma = 5/3$, the following expression is obtained for $\sigma = 0.72$

$$\beta_1 = 1.59 \left[1 + \frac{0.802 W}{ZW - 1} \left(1 + \frac{2.24}{W} \right) \right] \quad (26b)$$

This agrees with the results in Table 1 to within 2 percent for $W \geq 2$.

The effect of variable ρ_μ in the boundary layer has been treated in Reference 13 for the case of air. It was found that G_o is related to the value of G_o found from a constant ρ_μ solution by

$$G_o = (C_{e,o})^{0.37} (G_o)_{\rho_\mu = \text{constant}} \quad (27)$$

where $C_{e,o} = (\rho_e \mu_e / \rho_w \mu_w)_0$. The exponent 0.37 correlated the numerical boundary layer solution for $4 \leq M_s \leq 14$, $p_\infty = 0.001, 0.01$ atmospheres, and $T_\infty = T_w = 522^\circ R$ (in Ref. 13) and should be valid for air in a low pressure shock tube. Equation (27) should also give reliable estimates for the effect of variable ρ_μ for gases other than air.† This leads to the following expression

$$\beta_1 = (C_{e,o})^{0.37} (\beta_1)_{\rho_\mu = \text{constant}} \quad (27)$$

† For weak shocks, $C_{e,o}^{0.37}$ is nearly one and the correction for variable ρ_μ is small. For strong shocks G_o depends primarily on $(f - \eta)_{\infty,o}$, which is obtained from an integration of the momentum equation $(Cf'')' + ff'' = 0$ where $C = \rho_\mu / \rho_w \mu_w$. The quantity C varies monotonically from 1 at the wall to $C_{e,o}$ at the edge of the boundary layer. Its effect should depend primarily on the value of $C_{e,o}$ and should not be a strong function of the nature of the gas.

for obtaining β_1 from values of β_1 found from constant μ boundary layer solutions. Equation (26b) then gives, for $\sigma = 0.72$ and $W \geq 2$,

$$\beta_1 = 1.59 C_{e,o}^{0.37} \left[1 + \frac{0.802 W}{ZW - 1} \left(1 + \frac{2.24}{W} \right) \right] \quad (28a)$$

where an ideal gas (constant γ) solution for the shock is assumed (due to the presence of Z). For strong shocks, where γ no longer equals the ideal value, Z approximately equals W . Hence, for strong shocks, Z can be replaced by W and Eq. (28a) becomes

$$\beta_1 = 1.59 C_{e,o}^{0.37} \left[1 + \frac{0.802 W}{W^2 - 1} \left(1 + \frac{2.24}{W} \right) \right] \quad (28b)$$

Results from Eq. (28b) for air are listed in Table 2. These agree within 2 percent with the exact values of β_1 (computed from Eqs. 17 and 22a) for $M_s \geq 4$. The agreement is within 1 percent for $M_s \geq 8$.

C. SUMMARY AND DISCUSSION OF RESULTS

Various estimates for β have been made. These will now be reviewed and compared.

The parameter β_o was found by assuming the free stream to be uniform and by finding l_m such that the excess mass flow through the boundary layer equalled the mass flow through the shock. This assumes that the relative velocity between wall and free stream is $u_w - u_{e,o}$. Near the contact surface, the relative velocity is actually u_w . Hence, β_o is too small (i. e., l_m is overestimated). For weak shocks u_w is nearly equal to $u_{e,o}$ and the error is very large.

In order to obtain an improved estimate for β , the variation of free stream conditions was taken into account and a local similarity boundary layer solution was employed. A numerical integration was required and the resulting values of β were denoted β_2 . Values of β_2 were obtained for an

ideal gas with $\gamma = 7/5$ and $5/3$, $\sigma = 1$, and $\rho\mu = \text{a constant across the boundary layer}$. The results are given in Table 1 and Fig. 6. As expected, β_2 is larger than β_0 . The difference is very marked near $W = 1$ since β_0 behaves like $\sqrt{W - 1}$ while β_2 behaves like $1/\sqrt{W - 1}$ as $W \rightarrow 1$. The latter behavior for β_2 is required in order that l_m be finite as $W \rightarrow 1$ (see Eq. 3). The infinite value of β_2 , at $W = 1$, could have been avoided if Roshko had taken the characteristic velocity to be u_w rather than $u_w - u_{e,o}$ in Eqs. (1b) and (1c).

The numerical integration to obtain β_2 is tedious and simplifications were introduced to permit a closed form integration. The resulting values of β were denoted β_1 . Values of β_1 , for $\sigma = 1$, $\gamma = 5/3$ and $7/5$, and $\rho\mu$ constant may be compared with the corresponding values of β_2 in Table 1 and Fig. 6. It is seen that β_1 is somewhat larger than β_2 for larger W and is smaller than β_2 for W near 1. The two agree within 8 percent for $\gamma = 5/3$ and 5 percent for $\gamma = 7/5$, except near $W = 1$, where the local-similarity solution itself is least accurate. Since β_1 is relatively simple to obtain, it will be used henceforth instead of β_2 to evaluate the flow in a low density shock tube.

Values of β_1 for air, including real gas effects and variable $\rho\mu$, are given in Table 2 and Fig. 7. The effect of variable $\rho\mu$ is to decrease β_1 by a factor $(C_{e,o})^{0.37}$. This effect is most pronounced for strong shocks and causes β_1 to decrease continuously with M_s . Figure 7 includes values of β_R (Eq. 5b), including real gas effects, as computed in References 8 and 14. The agreement between β_R (from Ref. 8) and β_1 near $M_s = 10$ is fortuitous, being due to a rough approximation by Roshko for the effect of $C_{e,o}$. The results of Reference 14, for β_R , are based on an accurate boundary layer solution. It is seen that β_R underestimates β_1 and therefore considerably overestimates l_m [recall $l_m \sim \beta^{-2}$] for the range of M_s in Fig. 7.

Values of β_1 for argon are included in Fig. 7. These were obtained by multiplying the values of β_1 in Table 1 ($\sigma = 0.72$, $\gamma = 5/3$) by $(C_{e,o})^{0.37}$. The normal shock solution for argon was based on $\gamma = 5/3$ and the results

Table 1. Evaluation of β_0 , β_1 , and β_2 Assuming Ideal Gas and Boundary Layer with $\rho\mu = \text{Constant}$.

W	M_s		$\sigma = 0.72$						$\sigma = 1.0$					
			$\gamma = 7/5$		$\gamma = 5/3$		$\gamma = 7/5$		$\gamma = 5/3$		$\gamma = 7/5$		$\gamma = 5/3$	
			β_0 †	β_1	β_0	β_1								
1.100	1.06	1.06	0.500	3.22	0.598	3.86	0.476	3.07	4.39	0.558	3.60	4.65		
1.221	1.13	1.15	0.704	2.69	0.831	3.18	0.671	2.56	3.19	0.777	2.97	3.36		
1.250	--	--	--	--	--	--	--	--	3.06	--	--	3.21		
1.500	1.29	1.34	0.957	2.32	1.11	2.68	0.913	2.22	2.49	1.04	2.51	2.56		
1.75	--	--	--	--	--	--	--	--	2.21	--	--	2.30		
2.000	1.58	1.73	1.18	2.12	1.34	2.39	1.13	2.02	2.08	1.25	2.24	2.15		
2.500	1.89	2.24	1.31	2.03	1.46	2.27	1.25	1.94	1.94	1.37	2.13	2.00		
3.000	2.24	3.00	--	--	--	--	1.33	1.89	1.87	1.44	2.05	1.92		
3.492	2.64	4.54	1.45	1.95	1.59	2.15	1.38	1.87	1.82	1.49	2.02	1.87		
4.000	3.16	∞	1.49	1.94	1.63	2.12	1.42	1.85	1.79	1.53	1.99	1.84		
5.000	5.00	--	--	--	--	--	1.49	1.83	1.75	--	--	--		
6.000	∞	--	1.60	1.89	--	--	1.53	1.81	1.73	--	--	--		

† Values of β_0 and β_1 are obtained from data in Table A-1.

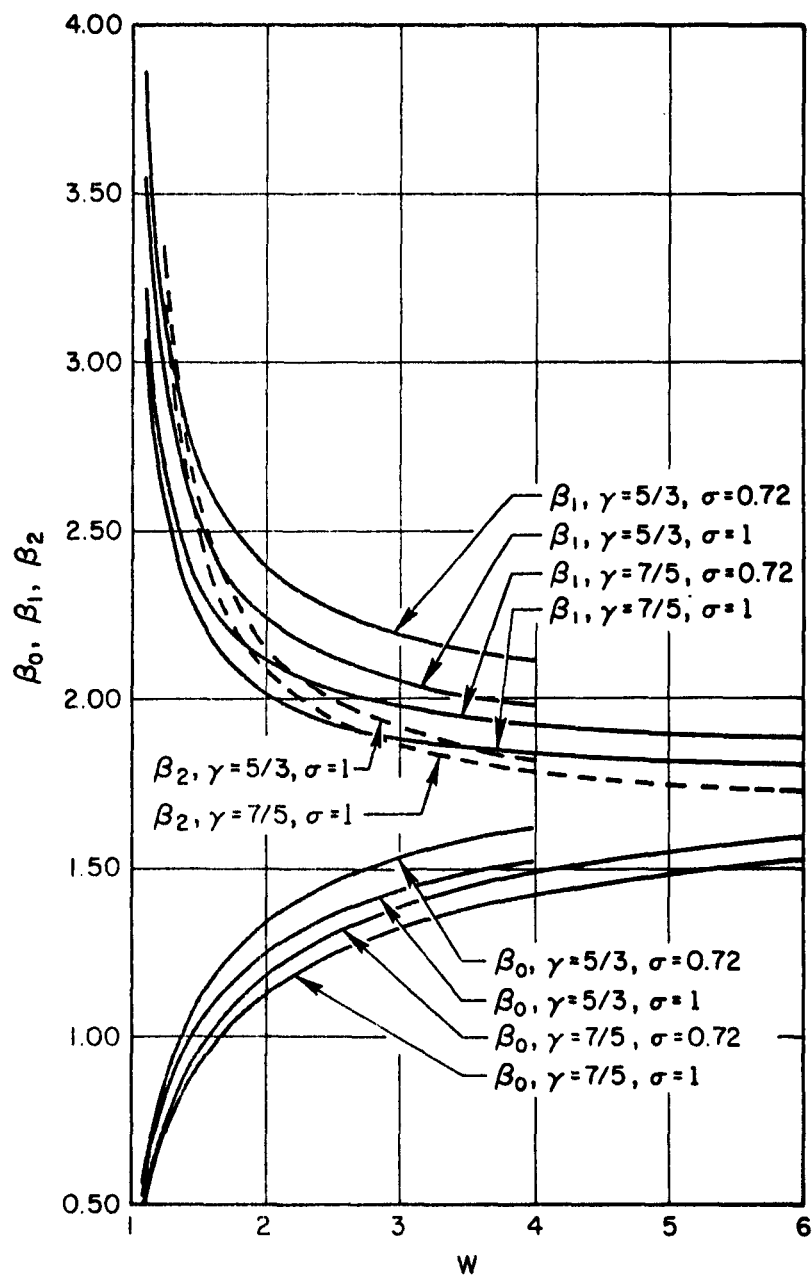


Fig. 6. Values of β for Ideal Gas With Constant γ , σ , and μ

Table 2. Values of β for Air Using Real Gas Boundary Layer Solution of Reference 13

$P_{\infty} = 0.001$ atm; $T_{\infty} = T_w = 522^{\circ}\text{R}$; $\sigma = 0.72$

M_s	W	$C_{e,o}$	$(f - \eta)_{\infty,o}$	$I_{\infty,o}$	G_o	β_o	β_1	Approx. β_1 (Eq. 28b)
4	4.875	0.641	1.584	0.2820	1.866	1.34	1.66	1.69
6	6.190	0.495	1.749	0.2537	2.003	1.24	1.47	1.45
8	8.060	0.406	1.951	0.2056	2.157	1.15	1.30	1.29
10	10.11	0.346	2.120	0.1658	2.286	1.07	1.19	1.18
12	10.93	0.299	2.102	0.1434	2.245	1.01	1.10	1.11
14	11.33	0.253	2.035	0.1264	2.161	0.951	1.04	1.04

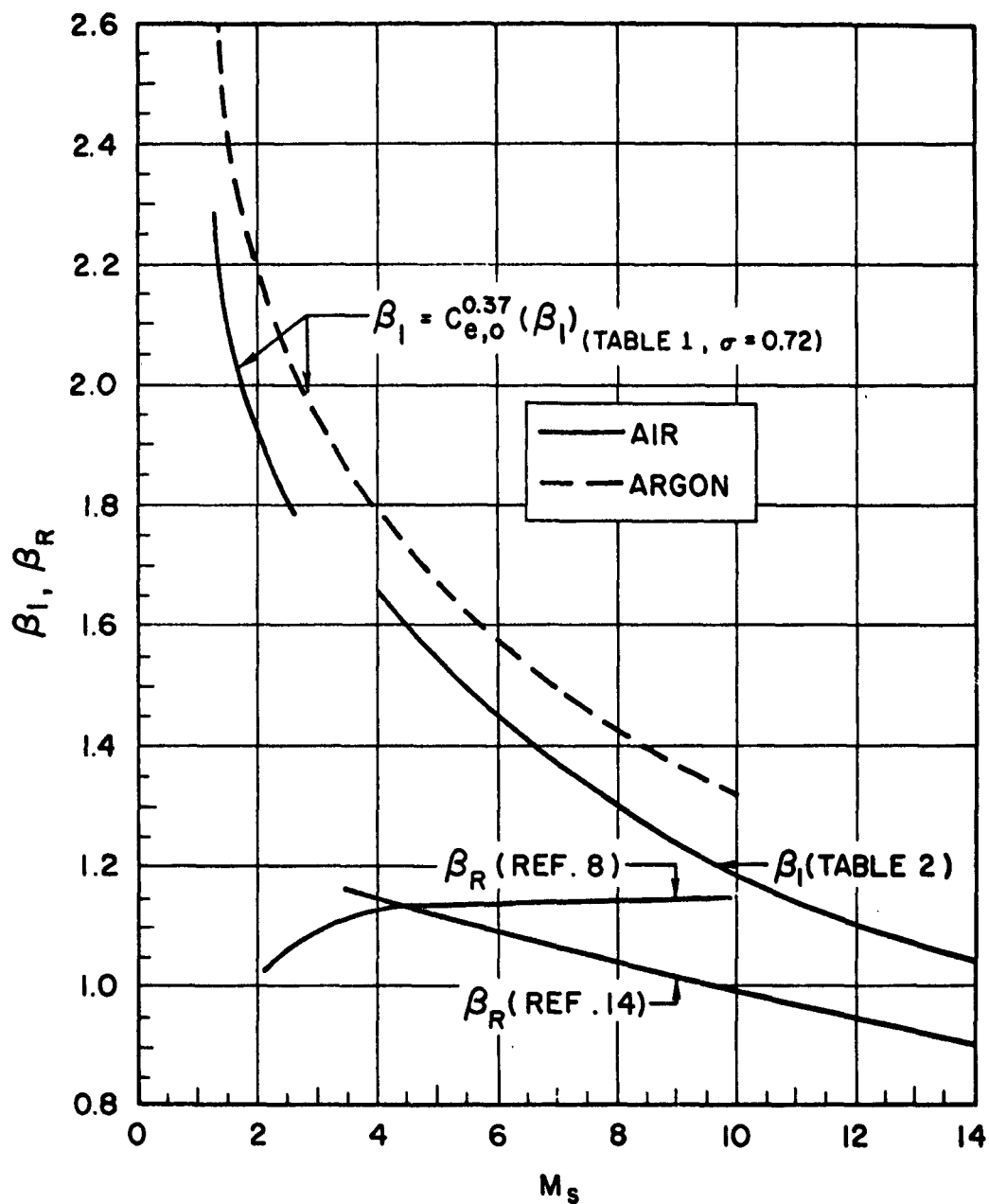


Fig. 7. Values of β for Air (Based on Equilibrium Real Gas Properties, $p_\infty \approx 0.001$ atm) and for Argon, Including Effect of Variable ρ ; $T_\infty = 522^\circ\text{R}$

are therefore not extended beyond $M_s = 10$ (where ionization effects become important).

Roshko⁸ measured test time in a low density shock tube for $2.5 \leq M_s \leq 9$ in air and argon. He found that $\beta = \sqrt{3}$ gave a mean correlation of the experimental data. However, since he computed β from Eqs. (5), he had no rational explanation of why β should be so high. The present results (Fig. 7) indicate that $\beta = \sqrt{3}$ is a reasonable mean value for his tests. The marked decrease of β with M_s indicates that smaller Mach number ranges should be used when correlating the experimental data, particularly for moderate M_s .

The present results for β_1 have been used in Eq. (3) to obtain the variation of $l_{mst}/d^2 p_\infty$ with M_s for air and argon. The results are given in Fig. 8. The standard condition in Eq. (3) was taken to be $T_{st} = 522^\circ R$ and $p_{st} = 1$ atmosphere, for which

$$\begin{aligned} \left(\frac{\rho a}{\mu}\right)_{st} &= 6.93 \times 10^6 \text{ ft}^{-1} && \text{air} \\ &= 7.39 \times 10^6 \text{ ft}^{-1} && \text{argon} \end{aligned}$$

Roshko used the values 6.74×10^6 and 7.03×10^6 for air and argon, respectively. These values correspond to a higher standard temperature [Note that $(\rho a/\mu)_{st} \sim T_{st}^{-1.26}$ for air, since $\mu \sim T^{0.76}$. The effect of initial temperatures other than $522^\circ R$ can be readily taken into account]. The results for air in Fig. 8 are based on values of β_1 obtained from Fig. 7 for $M_s \leq 14$ and on values obtained from Eq. (28b). Real gas normal shock solutions were employed. The difference in the values of l_{mst} for $p_\infty = 0.5$ cm and $p_\infty = 0.001$ cm is due to the effect of initial pressure on the shock solution. This difference is small and probably within the accuracy of the present solution. The results for argon in Fig. 8 are based on the values of β_1 in Fig. 7 and an ideal gas normal shock solution ($\gamma = 5/3$).

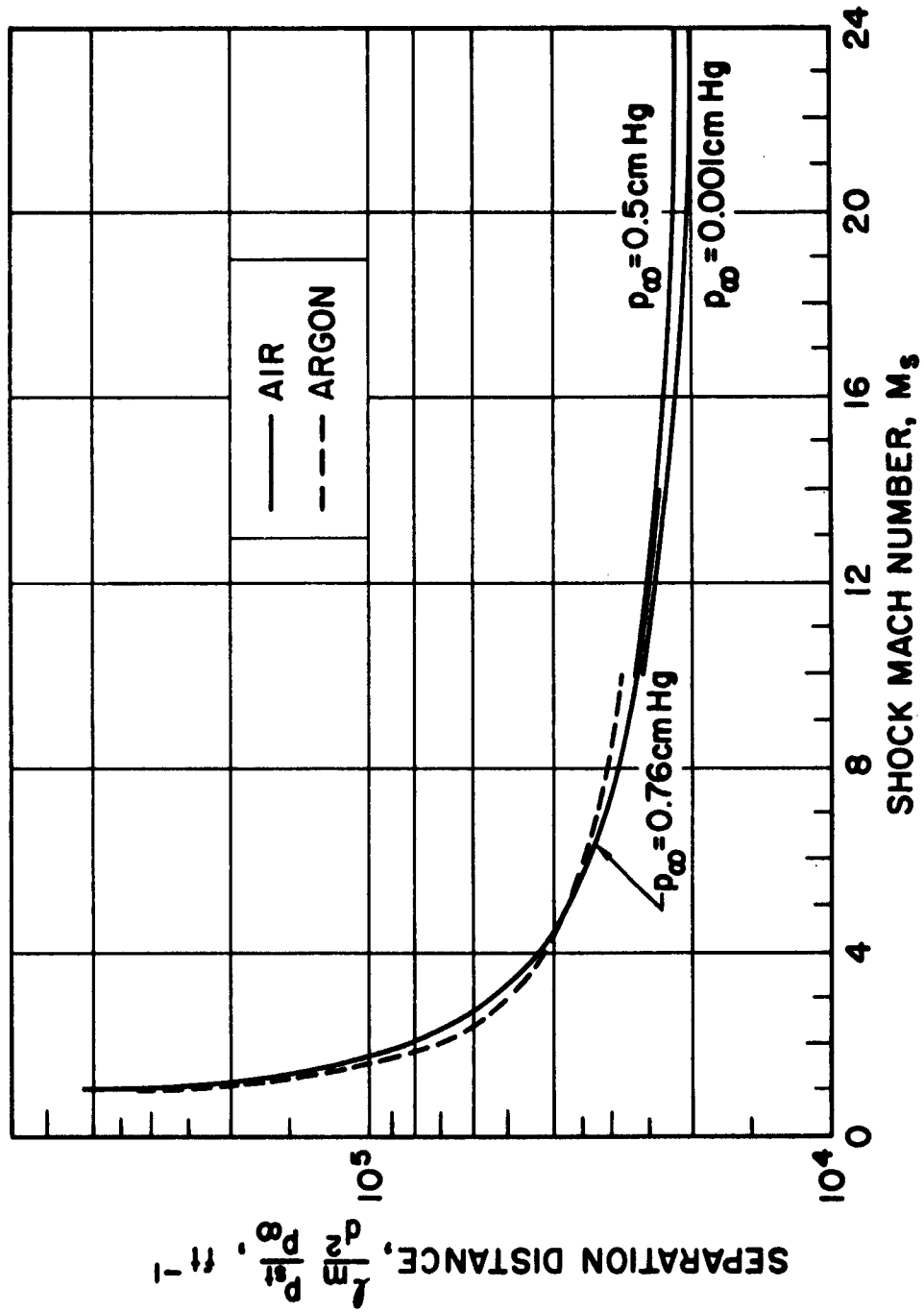


Fig. 8. Separation Distance for Air and Argon Including Effect of Variable μ :
 $T_\infty = 522^\circ\text{R}$, $P_{st} = 76 \text{ cm Hg}$

III. UNSTEADY SOLUTION

In the previous section, the asymptotic value of the separation distance between the shock and contact surface was found. This defines the test time in shock tubes that are sufficiently long to permit the asymptotic steady state flow to be reached. The separation distance as a function of time is required in order to estimate test times in shock tubes wherein the steady state solution is not achieved. This problem is now discussed.

It is desired to find the separation distance as a function of time, t , assuming that the shock and the contact surface are coincident at $t = 0$. This problem is very difficult to solve, and it is necessary to set up an approximate model for the flow. Two limiting approaches seem tractable. The first is to assume that the contact surface moves with uniform velocity and to attempt to compute the nonuniform motion of the shock relative to the contact surface. At first glance, References 8 and 10 appear to use this approach. However, in both of these references it is assumed that the mass flow through the shock, \dot{m}_s , is a constant and thus a uniform shock velocity is implicitly assumed. In addition, the proper boundary layer theory to be used in the contact surface fixed co-ordinate system is not clear. (In Refs. 8 and 10 attempts are made to relate the boundary layer to that behind a constant velocity shock with a uniform free stream downstream of the shock.) The second approach is to assume that the shock moves with uniform velocity and to find the rate at which the contact surface moves relative to the shock. This model can be specified more precisely than the first one, is self-consistent, and leads naturally to the asymptotic solution obtained in the previous section. The latter model will be treated herein.

A. SEPARATION BETWEEN SHOCK AND CONTACT SURFACE

Consider flow in a co-ordinate system in which the shock is fixed and the wall moves with velocity u_w . Assume that at time $t = 0$ the contact surface coincides with the shock and that at some later time, t , the portion of the

contact surface which is in the free stream is located at l (Fig. 9). Also assume that the flow between the shock and the contact surface is steady.

For steady flow, the rate of mass flow through the shock equals the rate of mass flow through a control surface at l . Thus

$$\begin{aligned} (\rho_e u_e)_o A &= \int \rho u \, dA \\ &= \rho_e u_e A + \rho_e u_e L (-\delta^*) \end{aligned} \quad (29)$$

where δ^* is the displacement thickness at l . This continuity equation can be reduced to

$$\bar{\delta} = 1 - \frac{\rho_e u_e}{(\rho_e u_e)_o} \quad (30)$$

which is the same as Eq. (8). If l is replaced by ξ (Eq. 10b), and local similarity is assumed for the boundary layer, it again follows (see derivation of Eq. 16) that

$$d\xi = 2\bar{\delta} d\bar{\delta} / H_e^2 \quad (31)$$

We are now interested in obtaining l as a function of t . But $dl/dt = u_e$. Thus $t = \int_0^l dl / u_e$. Define $X \equiv u_{e,o} t / l_m$, $T \equiv l / l_m$. It then follows (from $l/l_m = \xi/\xi_m$ and Eq. 31) that

$$X \equiv \frac{u_{e,o} t}{l_m} \equiv \frac{x_s}{W l_m} = \frac{\int_0^{\bar{\delta}} \bar{\delta} d\bar{\delta} / (V H_e^2)}{\int_0^1 \bar{\delta} d\bar{\delta} / H_e^2} \quad (32a)$$

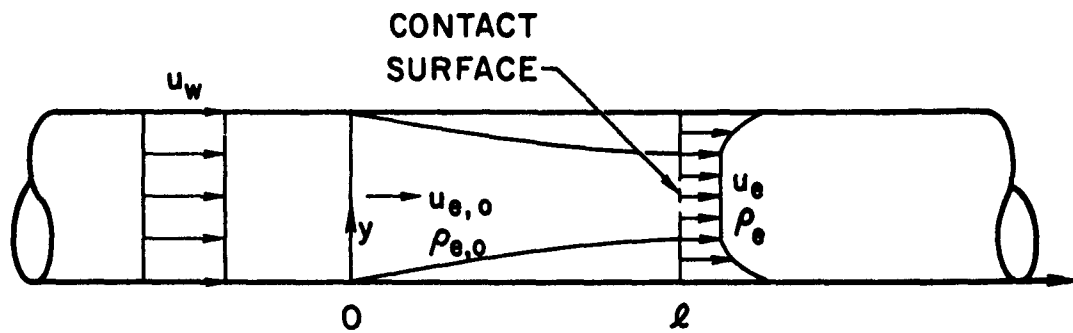


Fig. 9. Flow Model for Finding Separation Distance Between Shock and Contact Surface as a Function of Time

$$T \equiv \frac{l}{l_m} = \frac{\int_0^{\delta} \delta d\delta / H_e^2}{\int_0^1 \delta d\delta / H_e^2} \quad (32b)$$

The quantity x_s in Eq. (32a) is the distance of the shock from the diaphragm, $x_s = u_w t$. Equations (32) give the separation distance l as a function of t (or x_s). The parameters X and T are the same as those introduced by Roshko. The quantity T is the ratio of the separation distance l to the asymptotic value l_m . The quantity X is the time t divided by the time it would take an ideal shock tube (no boundary layer) to achieve a separation distance l_m . The latter may also be viewed as the shock distance x_s divided by the distance required, in an ideal shock tube, to achieve a separation distance l_m . Note also that $dT/dX = u_e / u_{e,0}$. For an inviscid flow, $X = T$. The departure of X from T is a measure of the wall boundary layer effect.

Equations (32) have been integrated for an ideal gas with $\sigma = 1$ and constant $\rho\mu$ across the boundary layer for $\gamma = 7/5$ and $5/3$. Equations (A-13) through (A-16) were used. Plots of X versus T are given in Fig. 10. The results for $W = 1.25$, $\gamma = 7/5$, and for $W = 1.25$, $\gamma = 5/3$, are sufficiently close that they appear as a single curve in Fig. 10. Similarly, the results for $W = 6$, $\gamma = 7/5$, and $W = 4$, $\gamma = 5/3$, appear as a single curve. The displacement between these curves is small and intermediate values of W are therefore not plotted.

A simpler relation between X and T , suggested by the solution for strong shocks, can be found as follows. Write Eq. (29) as

$$l = \frac{\rho_e u_e}{(\rho_e u_e)_0} + \frac{\rho_e u_e L(-\delta^*)}{(\rho_e u_e)_0 A} \quad (33)$$

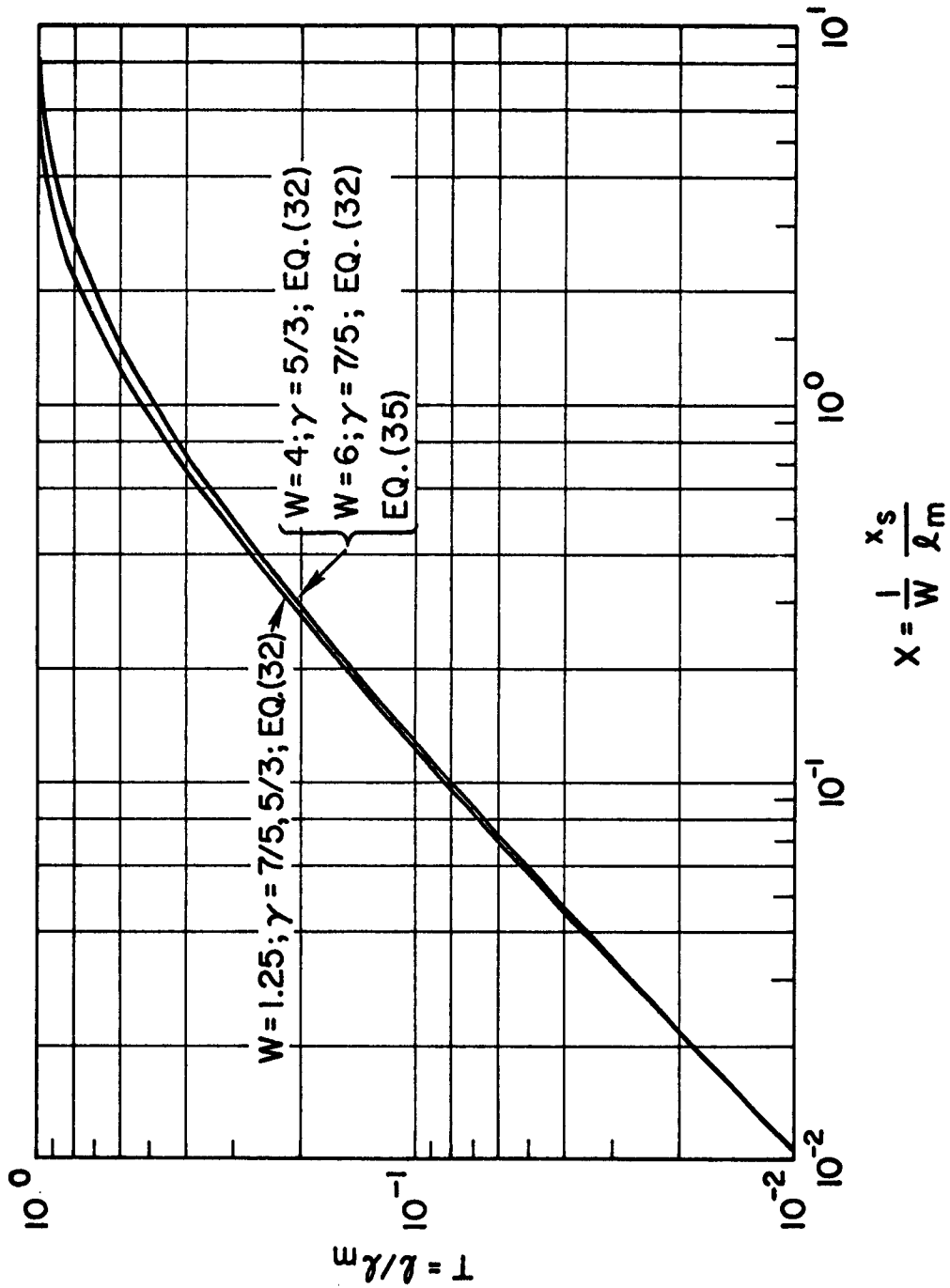


Fig. 10. Variation of T With X From Numerical Integration of Eq. (32) (For Ideal Gas, $\sigma = 1$, and $\rho\mu = \text{Constant}$) and From Eq. (35)

If variations in free stream density are neglected, the first term on the right hand side can be written as $u_e/u_{e,0} = dT/dX$. The second term on the right hand side is the ratio of the excess mass flow through the boundary layer at l to the mass flow through the boundary layer at l_m . For strong shocks, the external free stream remains fairly uniform and the excess mass flow in the boundary layer grows approximately as \sqrt{l} so that the second term can be approximated by $\sqrt{l/l_m} = \sqrt{T}$. Equation (33) then becomes

$$1 = \frac{dT}{dX} + \sqrt{T} \quad (34)$$

This is the same equation as that derived by Roshko and the solution is

$$-\frac{X}{Z} = \ln(1 - \sqrt{T}) + \sqrt{T} \quad (35)$$

Equation (35) is also plotted in Fig. 10 and is indistinguishable from the previous results for $W = 6$, $\gamma = 7/5$, and $W = 4$, $\gamma = 5/3$. This shows that the plot of X versus T is relatively insensitive to W and γ and that Eq. (35) gives an accurate representation except for W very near 1.

B. TEST TIME

In the previous calculation, the separation distance was obtained as a function of t . A quantity that is perhaps of greater interest is the test time (i. e., the difference in time between the arrival of the shock and the arrival of the contact surface) at a fixed value of x . This quantity will now be discussed.

Designate the test time by τ . For $t \rightarrow \infty$, $\tau = l_m/u_w$. Define $\bar{\tau} \equiv u_w \tau/l$, which is the test time at x divided by the test time at $x \rightarrow \infty$. Since $u_w - u_e$ is the velocity of the contact surface relative to the shock tube wall, the test time will nearly equal $l/(u_w - u_e)$. Also, $u_{e,0} \geq u_e \geq 0$. It then follows that

$$\frac{W}{W-1} T \geq \bar{\tau} \geq T \quad (36)$$

At the start of the motion, $\bar{\tau} = WT/(W - 1)$, whereas after long times $\bar{\tau} = T$. If W is large, $\bar{\tau} = T$ throughout the entire motion.

The test time $\bar{\tau}_a$ at a particular station x_a is found analytically as follows. In the present model, the shock moves with uniform velocity u_w . Let l_a be the separation distance when the shock is at x_a , and let x_b be the location of the shock when the contact surface is at x_a . From Fig. 11 it is clear that $x_a = x_b - l_b$ and $\tau_a = t_b - t_a = l_b/u_w$. In nondimensional variables, the latter expressions become

$$X_a = X_b - T_b/W \quad (37a)$$

$$\bar{\tau}_a = T_b \quad (37b)$$

Equations (37) give corresponding values of X_a and $\bar{\tau}_a$ from corresponding values of X_b and T_b (which are found from Eqs. (32) or Fig. 10). Since station a is arbitrary, the subscript a may be removed from Eqs. (37). Plots of $\bar{\tau}$ versus X are given in Fig. 12 for an ideal gas, where $\sigma = 1$ and $\rho\mu = \text{constant}$.

If Eq. (35) is used, the relation between X and $\bar{\tau}$ becomes

$$-X = 2[\ln(1 - \sqrt{\bar{\tau}}) + \sqrt{\bar{\tau}}] + \bar{\tau}/W \quad (38)$$

Equation (38) is also plotted in Fig. 12.

It is seen from Fig. 12 that the variation of $\bar{\tau}$ with X is more sensitive to W than is the variation of T with X (Fig. 10.) Equation (38) gives a reliable estimate for the variation of $\bar{\tau}$ with X except for W near 1.

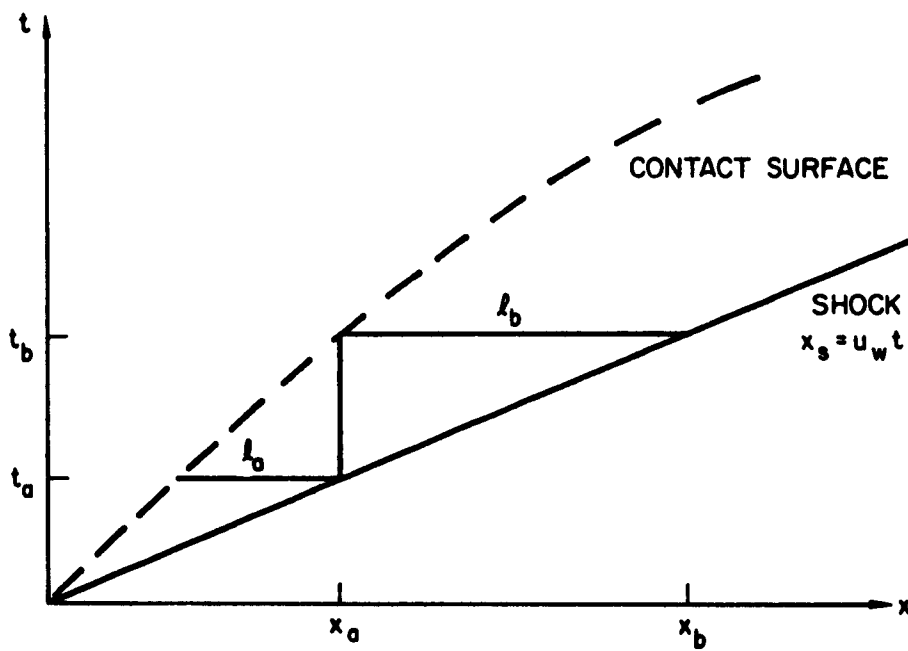


Fig. 11. Determination of Test Time at x_a

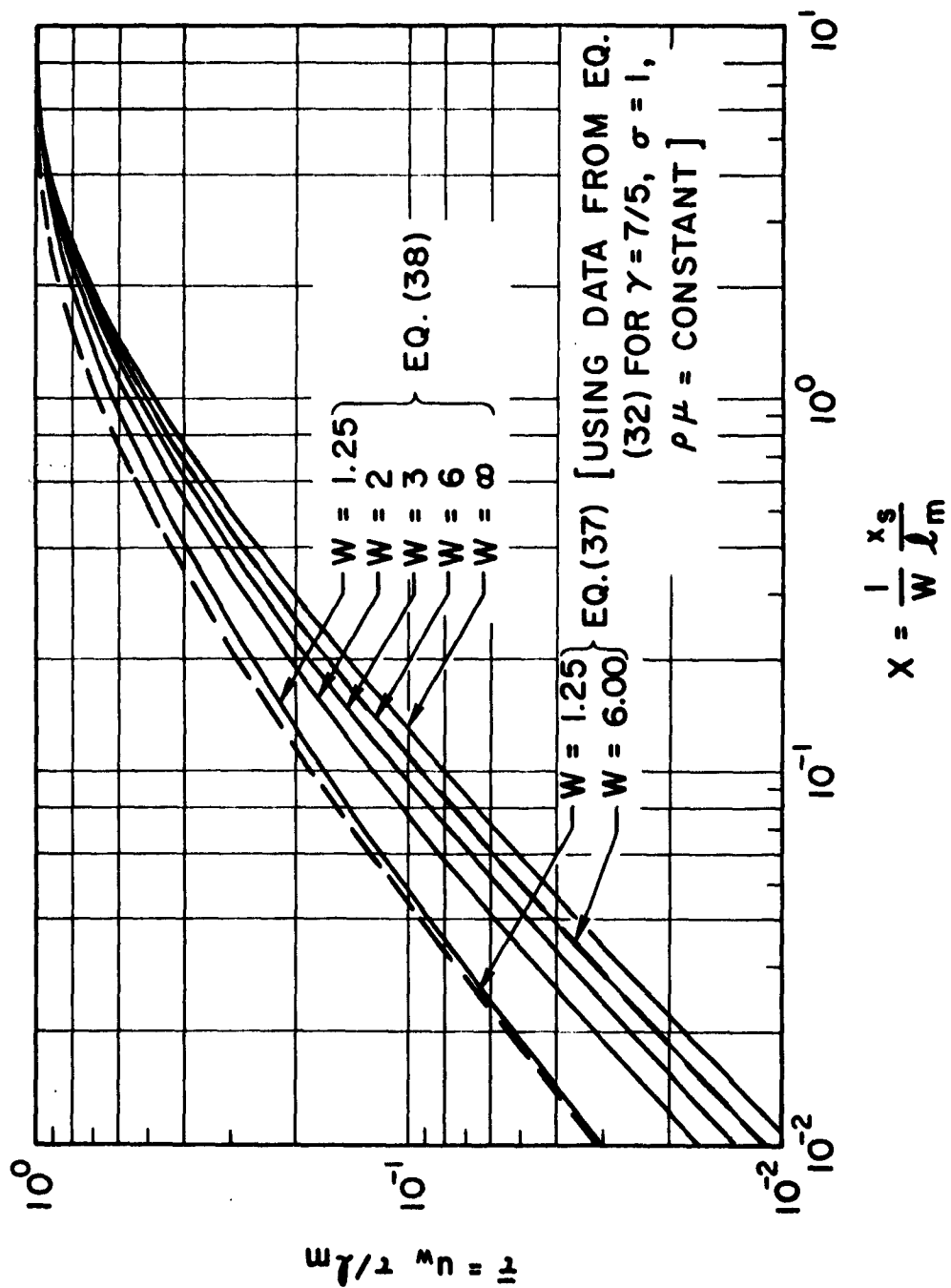


Fig. 12. Test Time at Given Station

Since the variation of T with X is relatively insensitive to W (compared with $\bar{\tau}$ versus X), it is preferable to attempt to correlate experimental data on the basis of T versus X . The data should then correlate with the single curve defined by Eq. (35) for all values of W except W near 1. Experimental observations of test time can be reduced to T as follows. If $\bar{\tau}_a$ is the nondimensionalized test time at X_a , Eq. (37) indicates that the corresponding values of T and X are

$$X = X_a + \bar{\tau}_a / W \quad (39a)$$

$$T = \bar{\tau}_a \quad (39b)$$

This reduction procedure becomes more important as W decreases. A similar procedure has been discussed in Reference 10.

IV. COMPARISON WITH REFERENCES 8 AND 10

References 8 and 10 used a contact surface fixed co-ordinate system to study the separation between the shock and the contact surface. The derivation of their basic equations is outlined here. The assumptions which are required to reduce the equations for the shock fixed model to those of References 8 and 10 are also noted and discussed.

The notation to be used in the contact fixed co-ordinate system is indicated in Fig. 13. Subscripts 1 and 2 denote conditions upstream and downstream of the shock, respectively. U_s is the velocity of the shock relative to the wall and u_2 is the velocity of the free stream in region 2 relative to the wall. In both References 8 and 10 it is assumed that the free stream is uniform in region 2 so that u_2 is a constant and also equals the velocity of the contact surface relative to the wall. Hence, the free stream velocity is zero in region 2 in contact surface fixed co-ordinates. The above notation is the same as that used in References 8 and 10. In addition, the velocity in the boundary layer, relative to the contact surface, will be denoted by \hat{u} (Fig. 13).

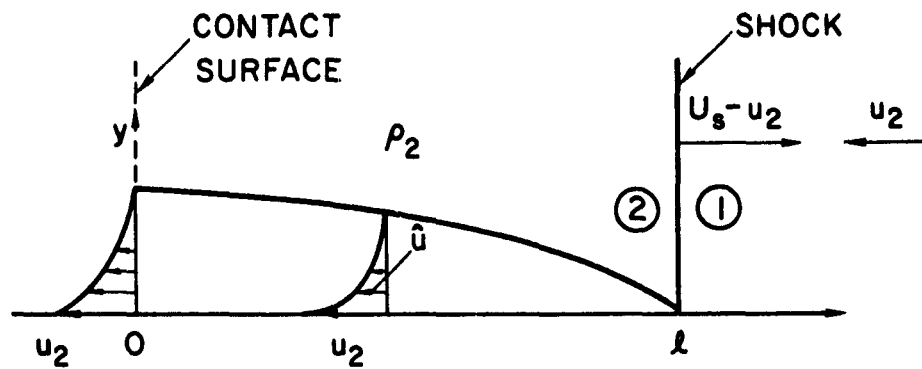
The mass balance between flow entering and leaving region 2 is found as follows. The rate at which mass enters the shock at any instant is

$$\dot{m}_s = \rho_1 U_s A = \rho_2 (U_s - u_2) A \quad (40)$$

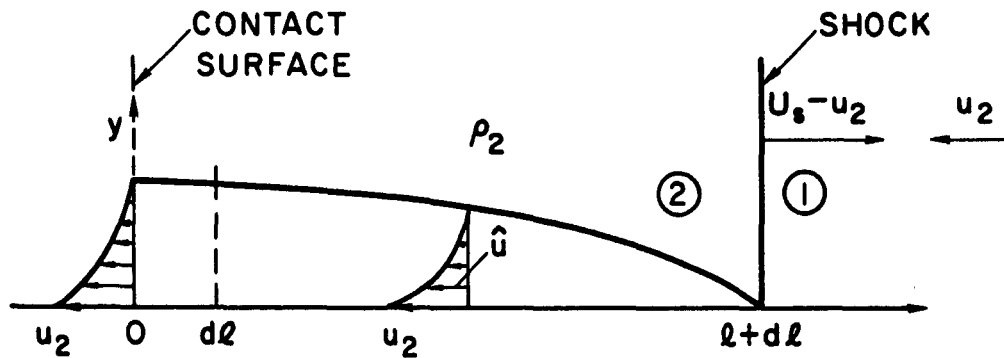
The rate at which mass leaves, at the plane of the contact surface, is

$$\dot{m}_c = L \int_0^{\infty} \rho \hat{u} dy \quad (41)$$

where $\rho \hat{u}$ is zero outside of the boundary layer. The rate of increase in mass between the shock and contact surface, \dot{m} , can be found in the following



(a) TIME t



(b) TIME $t + dt$

Fig. 13. Flow in Contact Surface Fixed Coordinate System of References 8 and 10

manner. Consider the interval of time between t and $t + dt$. The separation distance increases by an amount $d\ell$. Assume that the mass between 0 and ℓ at time t is the same as the mass between $d\ell$ and $\ell + d\ell$ at time $t + dt$ (see Fig. 13). The increased mass between the shock and contact surface is then contained between stations 0 and $d\ell$ and equals

$$\begin{aligned} dm &= \left(\int \rho \, dA \right) d\ell \\ &= \left[\rho_2 A + L \int_0^{\infty} (\rho - \rho_2) \, dy \right] d\ell \end{aligned} \quad (42)$$

This gives the following expression for the rate of increase of mass in region 2:

$$\dot{m} = \left[\rho_2 A + L \int_0^{\infty} (\rho - \rho_2) \, dy \right] \frac{d\ell}{dt} \quad (43)$$

(Roshko used $\dot{m} = \rho_2 A \, d\ell / dt$ and Hooker used the integral in the form $\int_0^{y_{bl}} \rho \, dy$. Reference 14 corrected Hooker's integral.) Continuity of mass, $\dot{m}_s - \dot{m}_c = \dot{m}$, then gives

$$(U_s - u_2) - \sqrt{\ell} \left(\frac{L}{A} \int_0^{\infty} \frac{\rho \hat{u}}{\rho_2 \sqrt{\ell}} \, dy \right) = \frac{d\ell}{dt} \quad \text{Roshko} \quad (44a)$$

$$= \frac{d\ell}{dt} \left[1 + \sqrt{\ell} \left(\frac{L}{A} \int_0^{\infty} \left(\frac{\rho}{\rho_2} - 1 \right) \frac{dy}{\sqrt{\ell}} \right) \right] \quad \text{Hooker} \quad (44b)$$

where the integrations are taken at the contact surface.

Since the free stream was assumed uniform in region 2, the integrals in Eq. (44) can be evaluated using the results of References 11 to 13 and are independent of l and t . Hence Eqs. (44) can be integrated to find l as a function of t . In integrating Eq. (44), both Roshko and Hooker assumed that $U_s - u_2$ is a constant. However, from Fig. 13, it is seen that $U_s - u_2 = dl/dt$ and therefore cannot be a constant for shock tube flows when the wall boundary layer effects are important. Hence there is an inconsistency in this model beyond the assumption of uniform flow in region 2. The assumption that $U_s - u_2$ is constant is equivalent to assuming that the mass flow rate through the shock is constant. This is precisely the basic assumption made in the shock fixed model and it is not unexpected that the two models give a similar variation of l with t .

Equations (44) can be put into shock fixed notation by letting $U_s - u_2 = u_{e,o}$, $\hat{u} = u - u_{e,o}$, and $\rho_2 = \rho_{e,o}$. The result is

$$1 - \frac{1}{u_{e,o}} \frac{dl}{dt} - \sqrt{l} \frac{L}{A} \int_0^{\infty} \frac{\rho}{\rho_{e,o}} \left(\frac{u}{u_{e,o}} - 1 \right) \frac{dy}{\sqrt{l}} = 0 \quad \text{Roshko (45a)}$$

$$= \frac{\sqrt{l}}{u_{e,o}} \frac{dl}{dt} \frac{L}{A} \int_0^{\infty} \left(\frac{\rho}{\rho_{e,o}} - 1 \right) \frac{dy}{\sqrt{l}}$$

Hooker (45b)

(Roshko used $\rho \hat{u} / \rho_2 = \rho u / \rho_{e,o} - u_{e,o}$ as well as $\rho \hat{u} / \rho_2 = \rho(u - u_{e,o}) / \rho_{e,o}$ and the former is the transformation error previously noted in connection with Eq. 5b.) The limit $dl/dt = 0$, in Eqs. (45), shows that the asymptotic separation distance l_m is obtained from a value of β

equal to β_R as defined in Eq. (5b). When put in terms of X and T, Eq. (45a) reduces to Eq. (34) and the integral is given by Eq. (35). However, in terms of X and T, Eq. (45b) becomes

$$1 - \frac{dT}{dX} - \sqrt{T} = \left[\frac{I_\infty}{(f-\eta)_\infty} \right]_0 \sqrt{T} \frac{dT}{dX} \quad (46)$$

which can be integrated to give

$$-\frac{X}{Z} = \left[1 + \frac{I_\infty}{(f-\eta)_\infty} \right]_0 \left[\ln(1 - \sqrt{T}) + \sqrt{T} \right] + \left[\frac{I_\infty}{(f-\eta)_\infty} \right]_0 \frac{T}{Z} \quad (47)$$

Equation (47) is Hooker's modification of Roshko's Eq. (35). The difference between these equations is small, particularly for strong shocks.

Equations (45) can be compared with the corresponding equations which arise in the shock fixed model. Equation (29) can be written

$$\begin{aligned} 1 - \frac{\rho_e u_e}{(\rho_e u_e)_0} - \sqrt{l} \frac{L}{A} \frac{\rho_e u_e}{(\rho_e u_e)_0} \int_0^\infty \frac{\rho}{\rho_e} \left(\frac{u}{u_e} - 1 \right) \frac{dy}{\sqrt{l}} \\ - \frac{\rho_e u_e}{(\rho_e u_e)_0} \sqrt{l} \frac{L}{A} \int_0^\infty \left(\frac{\rho}{\rho_e} - 1 \right) \frac{dy}{\sqrt{l}} = 0 \end{aligned} \quad (48)$$

This can be reduced to Eqs. (45) by taking $\rho_e = \rho_{e,0}$ and by taking u_e equal to either $u_{e,0}$ or dl/dt , depending on the particular term involved. If $u_e = u_{e,0}$ in the third term of Eq. (48), and if $u_e = dl/dt$ in the fourth term, Eq. (48) reduces to Hooker's Eq. (45b). However, it is more consistent to let $u_e = u_{e,0}$ for both these terms. This would mean that the coefficient $(dl/dt)/u_{e,0}$ on the right hand side of Hooker's Eq. (45b) could be replaced

by 1. If this substitution is made in Eq. (45b) then it would yield a value of β defined by β_0 (which is more accurate than β_R) and a variation of T with X as given by Roshko's Eq. (35). The latter was shown in Fig. 10 to be in good agreement with the integral solution of the shock fixed model for all W except W near 1.

Hence Hooker's relatively small correction (Eq. 47) to Roshko's result (Eq. 35) for the variation of T with X does not appear warranted. Equation (35) is sufficiently accurate, considering the basic limitations of the contact surface fixed model. The major problem is that of accurately determining β .

V. COMPARISON WITH EXPERIMENTAL DATA

Experimental observations of test time in low pressure shock tubes are reported in References 7, 8, 10, and 15. The results of the first three of these papers are summarized in Fig. 14. The results will be considered in the light of the present study. In particular, the question of whether the use of β_1 leads to improved correlations will be investigated.

The experimental results in Fig. 14 were reduced on the basis of $\beta = \sqrt{3}$ and $T = \bar{\tau}$.[†] The value of $\beta = \sqrt{3}$ was chosen by Roshko as a mean fit to his experimental data. Recall that both X and T are multiplied by β^2 (since $l_m \sim \beta^{-2}$). An increase in β will result in an increase in both X and T. In regions where T has reached its asymptotic value (i. e., is independent of X), changes in β will raise or lower T, but the effect on X will be unimportant with regard to correlation with the asymptotic portion of the theoretical curve in Fig. 14. If β were correctly evaluated, the experimental data should be asymptotic to $T = 1$. Hence, the asymptotic data can be used to evaluate β . In particular, $\beta = \sqrt{3/T_A}$ where T_A is the asymptotic value of T in Fig. 14 for the data in question.

The results of the above procedure are compared in Table 3 with values of β_1 from Fig. 7. For air in the range $M_g = 5$ through 9, β_1 is too small by about 10 percent. The results for argon cover three Mach number ranges and are more complete. It is seen that β_1 is too small by about 35 percent for $M_g = 1.6$, 20 percent for $M_g = 4$, and 10 percent for $M_g = 5$ through 9. These figures are only approximate, due to uncertainty and scatter in the experimental

[†]The quantity $\bar{\tau}$ was found from an experimental measurement of test time. The procedure noted in Eqs. (39) should be used to reduce the data to obtain a plot of T versus X. This would displace the points in Fig. 14 to the right. This displacement is unimportant in the region where T is near its asymptotic value, which is the region of primary concern here.

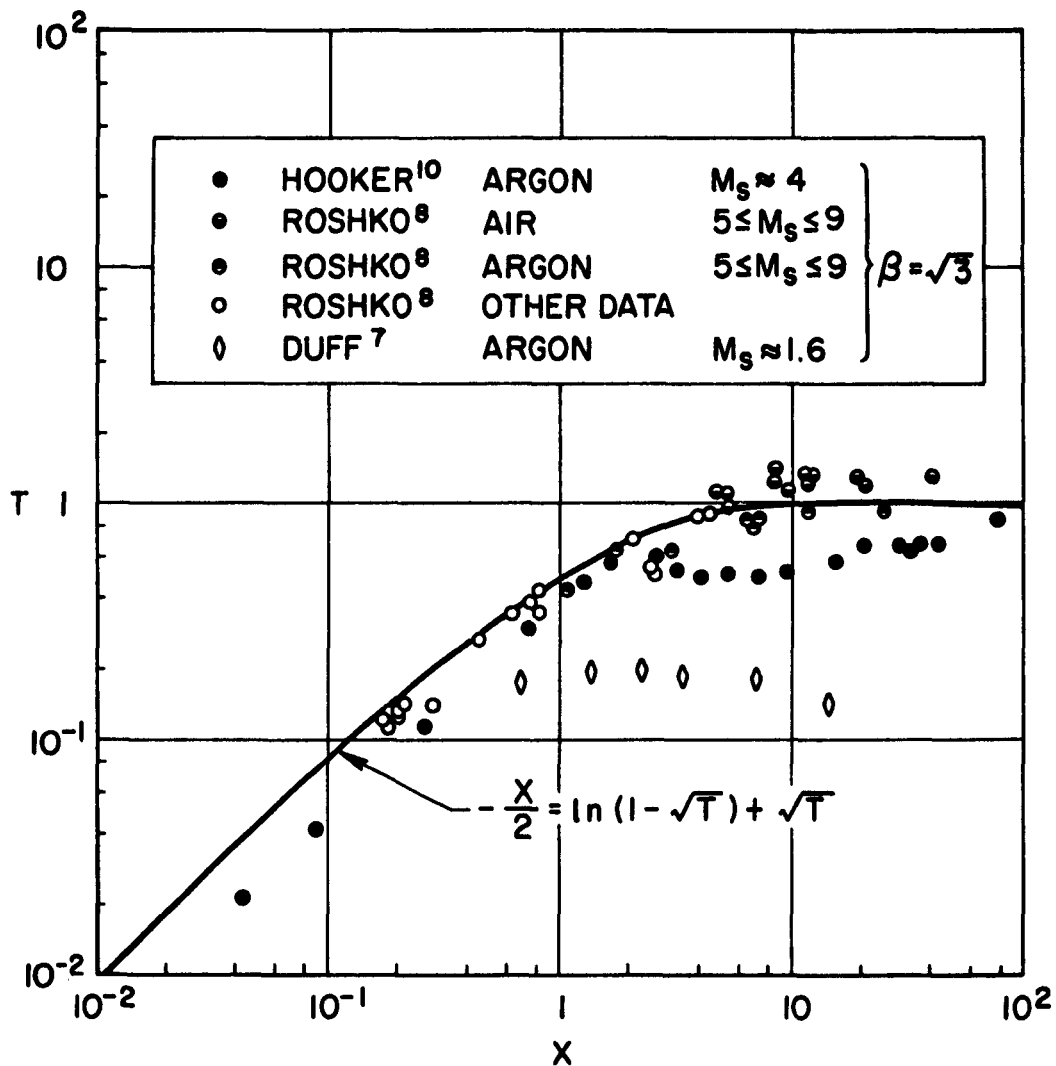


Fig. 14. Experimental Results of References 7, 8, and 10, Reduced on the Basis of $\beta = \sqrt{3}$ and $T = \bar{\tau}$ (Modified From Fig. 3, Ref. 10)

data. However, the trend appears reasonable in view of the fact that the procedures used to obtain β_1 and β_2 , in the present analysis, become more accurate as M_g increases. Mixing and diffusion at the contact surface would also tend to yield experimental values of β which are somewhat larger than β_1 . The magnitude of β_1 , and its variation with M_g , is in much better agreement than would be obtained by using β_R . The large values of β , as $M_g \rightarrow 1$, indicate that in the low M_g range the test time is much less than previous estimates based on β_R .

On the basis of the above data, it appears that the present estimates for β_1 are correct to about 10 percent for $M_g \geq 5$. Additional experimental data are required to better define β . A narrow range of M_g must be used when β is evaluated experimentally in the low M_g range.

Table 3. Evaluation of β from Experimental Data in Fig. 14

Gas	Ref.	M_g	T_A (Approx.)	$\beta = \sqrt{3/T_A}$	β_1 (Fig. 7)
Argon	7	1.6	0.2	3.9	2.4
Argon	10	4	0.6	2.2	1.8
Argon	8	5-9	0.9	1.8	1.7 - 1.4
Air	8	5-9	1.3	1.5	1.6 - 1.2

VI. ADDITIONAL CONSIDERATIONS

The present theory can be used to estimate the flow nonuniformity in low pressure shock tubes. In addition, the asymptotic shock strength for given initial shock tube conditions can be estimated. Since in the present theory a laminar wall boundary layer is assumed, it is also of interest to discuss transition to a turbulent boundary layer. Finally, it has been assumed that the boundary layer is thin compared with the tube diameter, and this assumption requires verification. These topics will now be briefly considered.

A. FLOW NONUNIFORMITY

An estimate of the flow nonuniformity between the shock and the contact surface can be obtained from Eq. (34), which, in dimensional variables, can be written

$$\frac{u_e}{u_{e,0}} = 1 - \sqrt{\frac{l}{l_m}} \quad (49)$$

This gives the variation of u_e with distance behind the shock. Isentropic flow relations can then be used to find the variation with l of all other flow properties. In shock fixed co-ordinates, the flow downstream of the shock corresponds to subsonic flow in an expanding channel. The density, temperature, and pressure increase with distance behind the shock. The net change in these properties can be expressed in terms of the flow Mach number directly behind the shock $u_{e,0}/a_{e,0}$ and is small for strong shocks. The present discussion neglects relaxation phenomena which may also contribute to variations in the free stream properties.

B. COMPARISON OF IDEAL AND ACTUAL ASYMPTOTIC SHOCK STRENGTH

The problem here is to estimate the actual asymptotic shock strength that will result from given initial conditions in a low pressure shock tube. Perfect gases with constant specific heats are considered. Here the conventional subscripts 1 and 4 are used to indicate initial conditions in the driven and driver sections, respectively.

If wall boundary layer effects are neglected, the resulting ideal shock Mach number $M_{s,i}$ is related to the initial pressure ratio p_4/p_1 and sound speed ratio a_4/a_1 by

$$\frac{Z_1 - 1}{Z_1(Z_4 - 1)} \frac{a_1}{a_4} \frac{M_{s,i}^2 - 1}{M_{s,i}} = 1 - \left(\frac{p_1}{p_4} \frac{(Z_1 + 1)M_{s,i}^2 - 1}{Z_1} \right)^{1/(Z_4 + 1)} \quad (50a)$$

In the derivation of Eq. (50a), it is assumed that the flow is uniform between the shock and contact surface.

Duff⁷ has pointed out that the ideal shock tube equations can be modified to account for the character of the asymptotic flow in a low pressure shock tube. In particular, Duff neglects the boundary layer effect in the driver gas (valid for strong shocks). He also assumes that the contact surface moves with the same velocity as the shock and that the pressure at the contact surface equals the stagnation pressure (relative to the shock) of the flow directly behind the shock. The shock Mach number $M_{s,A}$ that then results from given initial conditions is found from⁷

$$\begin{aligned} \frac{M_{s,A}}{Z_4 - 1} \frac{a_1}{a_4} = 1 - \left(\frac{p_1}{p_4} \frac{(Z_1 + 1)M_{s,A}^2 - 1}{Z_1} \right)^{1/(Z_4 + 1)} \\ \times \left(1 + \frac{M_{s,A}^2 + Z_1 + 1}{(Z_1 - 1)[(Z_1 + 1)M_{s,A}^2 - 1]} \right)^{(Z_1 + 1)/2(Z_4 + 1)} \end{aligned} \quad (50b)$$

The quantity $M_{s,A}$ may be termed the actual asymptotic shock strength. Eq. (50b) differs in form from Eq. (4) in Reference 7, since Duff was primarily interested in determining the initial pressure ratio p_4/p_1 required to achieve a given shock strength $M_{s,A}$.

When the shock tube diaphragm first bursts, the boundary layer effects are small and the shock Mach number will tend to be $M_{s,i}$ as given by Eq. (50a). Hence, $M_{s,i}$ may also be viewed as the initial shock Mach number. (The finite time required to rupture the diaphragm tends to alter this result somewhat). If the flow reaches its steady asymptotic limit, the shock Mach number is given by Eq. (50b). These two Mach numbers can be readily compared for large initial pressure ratios. In the latter case, Eqs. (50a) and (50b) can be equated to yield

$$\frac{M_{s,A}}{M_{s,i}} = \frac{W_i - 1}{W_i} \left[1 + O(p_1/p_4)^{1/(Z_4+1)} \right] \quad (51)$$

where W_i is the density ratio across the shock corresponding to $M_{s,i}$. For strong shocks, $M_{s,A}$ is only slightly less than $M_{s,i}$. The difference becomes more pronounced for weaker initial shocks.

Roshko⁸ has deduced an expression similar to Eq. (51) from a simple physical argument. Namely, for ideal flow, the shock velocity relative to the wall is $U_{s,i} = (W u_{e,o})_i$. For the asymptotic flow, the shock velocity approximately equals the ideal contact surface velocity relative to the wall; $U_{s,A} = (U_s - u_{e,o})_i$. The latter expressions give Eq. (51).

C. TRANSITION

It has been assumed throughout that the wall boundary layer is laminar between the shock and the contact surface. This assumption is generally valid for low pressure shock tubes. It is of interest to compute the Reynolds number at the contact surface for the asymptotic flow condition. If this is below the transition Reynolds number, then the validity of the laminar flow assumption is established.

In Reference 16, a transition Reynolds number defined by

$$(Re)_t = \frac{u_{e,o} [W - 1]^2 l_t}{\nu_{e,o}} \quad (52)$$

has been proposed for correlating transition in shock tubes. Here, l_t is the distance between the shock and the transition point. (The characteristic velocity used to deduce Eq. (52) is the flow velocity relative to the wall and the characteristic distance is the distance a particle moves in the free stream from the instant it is set into motion to the instant it is at the transition point.) Experimental observations of $(Re)_t$ are summarized in References 16 and 17. For weak shocks, $(Re)_t = O(10^6)$. The value of $(Re)_t$ increases with M_s , particularly for strong shocks where the low wall-to-free-stream temperature ratio tends to stabilize the boundary layer. This stabilization seems to occur at about $T_w/T_{e,o} \approx 0.1$, which corresponds to $M_s \approx 10$ in air. The data in Reference 17 indicates that for $1 \leq M_s \leq 9$, $(Re)_t$ appears to be in the range $0.5 \leq (Re)_t \times 10^{-6} \leq 4$. For larger M_s the values of $(Re)_t$ tend to increase markedly and values as high as 10^7 and 5×10^7 have been observed¹⁷ for M_s around 10. An analytical study of the stabilizing effect of low $T_w/T_{e,o}$ has been presented in Reference 18. The latter study is consistent with the experimental data for very weak shocks, but indicates infinite stability for $M_s > 2.18$ in air.

The Reynolds number at the contact surface, corresponding to a shock-contact surface separation distance of l_m , can be used to determine whether or not the laminar boundary layer assumption is correct. This Reynolds number is $(Re)_{l_m} = u_{e,o} [W - 1]^2 l_m / \nu_{e,o}$ assuming a uniform free stream, and can be put in the form

$$\left(\frac{p_{st}}{p_{\infty}} \right)^2 \frac{(Re)_{l_m}}{d^2} = M_s (W - 1)^2 \frac{\mu_w}{\mu_{e,o}} \left(\frac{\rho a}{\mu} \right)_{st} \left(\frac{l_m}{d^2} \frac{p_{st}}{p_{\infty}} \right) \quad (53)$$

The right hand side depends primarily on M_s . For a given M_s , $(Re)_{l_m}$ varies as $(dp_{\infty}/p_{st})^2$.[†] If d is increased to increase l_m , then smaller values of p_{∞} may be required in order to assure laminar flow. Eq. (53) has been evaluated, employing the same data as used to obtain Figs. 7 and 8, and the results are presented in Fig. 15.

The present results have been used to estimate $(Re)_{l_m}$ for one series of Roshko's tests in air. These tests were made in a tube with $d = 1/6$ feet, $5 \leq M_s \leq 9$ and $0.1 \text{ mm Hg} \leq p_{\infty} \leq 5 \text{ mm Hg}$. Using an average value $(p_{st}/p_{\infty})^2 (Re)_{l_m}/d^2 = 2 \times 10^{13}$ (from Fig. 15), it is found that $10^4 \leq (Re)_{l_m} \leq 2 \times 10^7$. At the higher values of $(Re)_{l_m}$, transition to a turbulent boundary layer might have occurred. This would reduce l_m , and increase the effective value of β , as compared with a completely laminar boundary layer.

D. BOUNDARY LAYER THICKNESS AT l_m

Let δ_u represent the value of y at which $(u_w - u)/(u_w - u_{e,o}) = 0.99$ and let η_u be the corresponding value of η . Hence, δ_u is a measure of the boundary layer thickness. Assuming that the flow behind the shock is uniform δ_u is given by (e. g., Ref. 13)

$$\delta_u = \left(\frac{p_w}{p_e} \sqrt{\frac{2l v_w}{u_e}} \right)_o [\eta_u - I_{\infty}]_o \quad (54)$$

The value of δ_u at l_m can be used as an index to determine whether the boundary layer thickness is small relative to the tube hydraulic radius $d/2$. Combining Eqs. (2) and (54) gives

$$\left(\frac{2\delta_u}{d} \right)_{l_m} = \frac{(\eta_u - I_{\infty})_o}{\beta \sqrt{2(W-1)}} \quad (55)$$

[†]This dependence is due to the fact that l_m varies as $d^2 p_{\infty}/p_{st}$ and the Reynolds number per unit length, behind the shock, varies as p_{∞}/p_{st} .

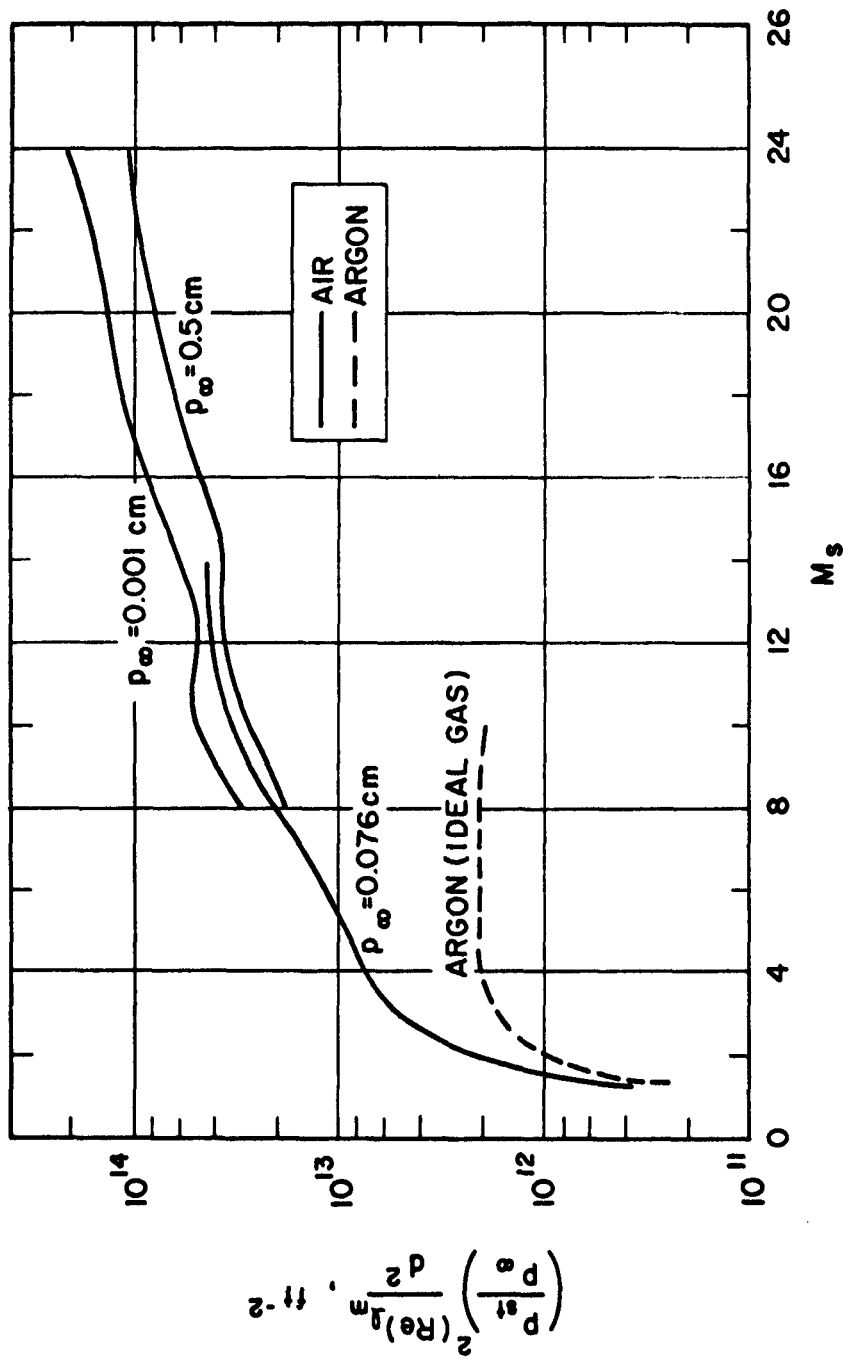


Fig. 15. Reynolds Number at Contact Surface (Eq. 53);
 $T_{\infty} = 522^{\circ}\text{R}$, $p_{st} = 76 \text{ cm Hg}$

For constant $\rho\mu$, it has been found¹³ that the interpolation formula $\eta_u = 3.20/\sqrt{1 + 0.543W}$ is accurate. This together with the values of I_∞ in Table A-1 permits Eq. (55) to be evaluated for constant $\rho\mu$. The effect of variable $\rho\mu$ on $(\eta_u - I_\infty)_0$ for air, has been determined in Reference 13. It was found that the variable $\rho\mu$ values of $(\eta_u - I_\infty)_0$ for air, can be obtained from the constant $\rho\mu$ values by multiplying the latter by $(C_{e,o})^{0.48}$. It may be assumed that the latter correction for variable $\rho\mu$ is also reasonable for other gases.

Values of $(2\delta_u/d)_{f_m}$ have been computed for air and for argon, including the effect of variable $\rho\mu$. It was assumed that $\beta = \beta_1$ in Eq. (55). The results are given in Fig. 16. It is seen that, for both argon and air, $(2\delta_u/d)_{f_m} \approx 1, 0.7$, and 0.4 for $M_g \approx 1.2, 1.6$, and 2.4 , respectively, and decreases with increase of M_g .

The excess mass flow in the boundary layer was previously found by integrations in which it was assumed that the boundary layer thickness small compared with d (e. g. , Eq. 6). Since most of this mass flow occurs in the portion of the boundary layer near the wall, δ_u is a conservative criterion for the size of the boundary layer relative to the tube radius. For laminar boundary layers, the thin boundary layer assumption is probably valid for M_g as low as about 1.6. This covers the range of M_g of practical interest in low pressure shock tubes.

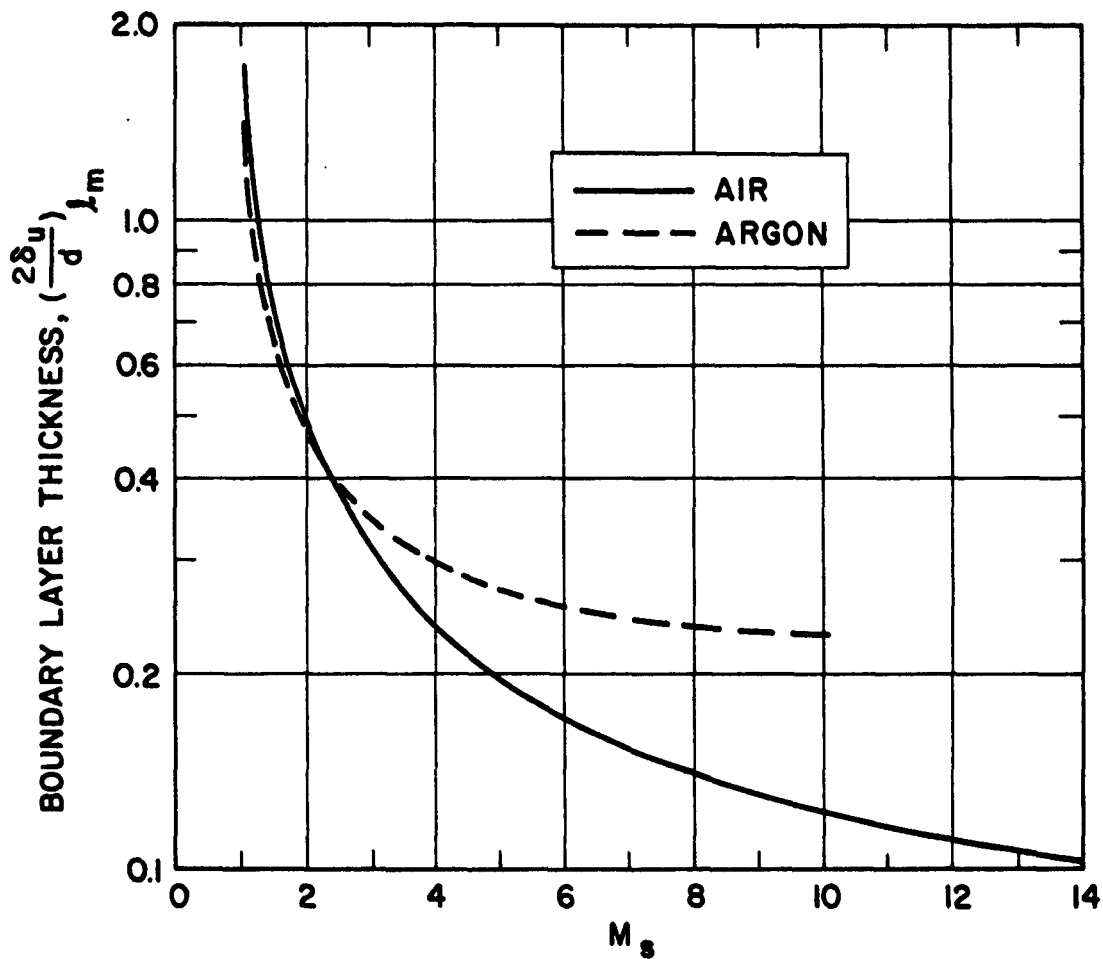


Fig. 16. Boundary Layer Thickness at l_m Corresponding to $(u_w - u)/(u_w - u_{e,o}) = 0.99$

VII. SUMMARY AND CONCLUDING REMARKS

Test time and flow nonuniformity in low pressure shock tubes have been investigated. It was assumed that the boundary layer was laminar and was thin relative to the tube diameter.

In the first portion of the study, the asymptotic flow after long times was considered. Here, the shock and contact surface moved with constant and equal velocity. The flow between shock and contact surface was steady, in a shock fixed co-ordinate system, and the separation distance was found. It was necessary to treat simultaneously the boundary layer development and the change in free stream conditions external to the boundary layer. A local similarity boundary layer solution was used which utilized the uniform free stream solutions given in References 11 to 13. The local similarity solution should be accurate except for M_g near 1 (where neglect of the pressure gradient on the boundary layer profile may become important). The accuracy of the local similarity solution can be established by more accurate solutions of the wall boundary layer or, perhaps, by applying the same procedure to boundary layer problems where the solutions are known. This has not been attempted.

The asymptotic separation distance yielded values of β which were considerably larger than the previous analytical estimates of Roshko and Hooker, particularly for moderate M_g . (As an example, consider $\gamma = 7/5$, $\sigma = 1$, and $\rho\mu$ constant across the boundary layer. Roshko obtained $0.91 \leq \beta_R \leq 1.52$, for $1.29 \leq M_g \leq \infty$, whereas we have obtained $2.22 \leq \beta_1 \leq 1.81$ for the same range of M_g .) Test time is proportional to β^{-2} . Hence, the previous analytical estimates for test time are much too large, particularly for moderate M_g .

The experimental test time data of Duff, Roshko, and Hooker indicated that the present estimates for β_1 , are still somewhat low. For argon, they are

too low by about 35 percent for $M_s = 1.6$; 20 percent for $M_s = 4$, and 10 percent for $5 \leq M_s \leq 9$. They are also about 10 percent low for $5 \leq M_s \leq 9$ in air. The discrepancy between theory and experiment decreases with increasing M_s . This trend is to be expected since the local similarity solution becomes more accurate as M_s increases. It is also to be expected that the analytical estimates for β_1 should be lower than the experimentally observed values since mixing and diffusion at the contact surface will tend to reduce test time (i. e., increase β).

In the second portion of the present paper, consideration was not restricted to the asymptotic flow, and the separation distance was found as a function of time. In order to make the problem tractable, it was assumed that the shock moved with uniform velocity and that the flow between the shock and the contact surface was steady (in shock fixed co-ordinates). Both assumptions are somewhat in error but should give at least qualitatively correct results. The variation of separation distance with time, in nondimensional form, was essentially the same as that obtained by Roshko, except for M_s near 1. Hence, the main difference between Roshko's results and the present results is in the numerical value of β^2 (which is used to nondimensionalize both separation distance and time).

The shock Mach number varies from an initial value of $M_{s,i}$ to an asymptotic value $M_{s,A}$ during the course of the flow in a low pressure shock tube. For strong shocks, $M_{s,i}$ nearly equals $M_{s,A}$ and the assumption of a uniform shock velocity is valid. For weaker shocks, the question might arise as to what value of M_s should be used to correlate experimental test time data or to theoretically predict test time. When correlating experimental data, the locally observed value of M_s should be used. When predicting test time, the local value of $X = x_s/Wt_m$ should first be evaluated using either $M_{s,i}$ or $M_{s,A}$ (Eq. 50). If $X \geq 0.10$, the local flow will be in the asymptotic flow condition, and $M_s = M_{s,A}$. If $X \leq 0.1$, the local flow is only slightly perturbed from the ideal flow, and $M_s = M_{s,i}$. For $X = 0(1)$, the local flow is in an intermediate condition and a mean value between $M_{s,i}$ and $M_{s,A}$ would be appropriate.

APPENDIX

BOUNDARY LAYER BEHIND MOVING SHOCK

The results given in References 11 and 12 are summarized with regard to the displacement thickness of the boundary layer behind a shock moving with uniform velocity. It is assumed that γ and σ are constant, that $\rho\mu$ is constant across the boundary layer, and that the free stream is uniform behind the shock.

These results are then put in a form applicable to the local similarity solution discussed in the body of the report.

UNIFORM FLOW BEHIND SHOCK

The boundary layer is indicated in Fig. 3. The free stream is uniform and is the same as that directly behind the shock. Subscript o is used for this flow.

In References 11 and 12 a similarity variable η is employed, defined by

$$d\eta = \sqrt{\frac{u_{e,o}}{2l_{v,w,o}}} \frac{\rho}{\rho_{w,o}} dy \quad (\text{A-1})$$

and a stream function $f_o(\eta)$ such that

$$f'_o = u/u_{e,o} \quad f_o(0) = 0 \quad (\text{A-2})$$

The boundary layer displacement thickness is given by

$$\delta^* = \int_0^{\infty} \left[1 - \frac{\rho u}{(\rho_e u_e)_o} \right] dy \quad (\text{A-3})$$

which is negative for the boundary layer behind a moving shock.

In terms of transformed quantities,

$$\begin{aligned}
 -\delta^* \frac{\rho_{e,o}}{\rho_{w,o}} \sqrt{\frac{u_{e,o}}{2I_{w,o}}} &= \lim_{\eta \rightarrow \infty} (f_o - \eta) + \int_0^{\infty} \left(1 - \frac{\rho_{e,o}}{\rho}\right) d\eta & (A-4) \\
 &\equiv [(f - \eta)_{\infty,o} + I_{\infty,o}]_o \\
 &\equiv G_o
 \end{aligned}$$

Equation (A-4) defines $(f - \eta)_{\infty,o}$, $I_{\infty,o}$, and G_o . These quantities are of fundamental importance in determining shock tube test time and can be evaluated from the numerical results given in References 11 through 13. Typical values are given in Table A-1 for fluids with constant specific heats, constant σ , and constant $\rho\mu$. Real gas results for air are given in Table 2.

The boundary layer parameters in Table A-1 were obtained as follows. The quantity $(f - \eta)_{\infty,o}$ is a function only of $W \equiv u_w/u_{e,o}$ and is tabulated in References 11 and 12. The quantity $I_{\infty,o}$ is found from¹¹

$$I_{\infty,o} = \frac{\gamma - 1}{2} M_{e,o}^2 (W - 1)^2 [r_o(0)I_{s,o} - I_{r,o}] + \left(1 - \frac{T_w}{T_{e,o}}\right) I_{s,o} \quad (A-5)$$

where $M_{e,o} = u_{e,o}/a_{e,o}$ and

$$I_{r,o} = \int_0^{\infty} r \, d\eta \quad I_{s,o} = \int_0^{\infty} s \, d\eta$$

The quantities $I_{r,o}$, $I_{s,o}$, and $r_o(0)$ are functions of σ , as well as W , and are defined and evaluated in References 11 and 12 for $\sigma = 0.72$. However, for $\sigma = 1$, these quantities become (using Ref. 11)

$$r_o(0) = 1 \quad I_{r,o} = \frac{(2W - 1)(f - \eta)_{\infty,o} + f_o''(0)}{(W - 1)^2} \quad I_{s,o} = \frac{(f - \eta)_{\infty,o}}{W - 1} \quad (A-6)$$

where $f''(0)$ is also a tabulated function of W . Normal shock relations give

$$\frac{\gamma - 1}{2} M_{e, o}^2 = \frac{1}{ZW - 1} \quad (\text{A-7a})$$

$$1 - \frac{T_w}{T_{e, o}} = 1 - \frac{T_\infty}{T_{e, o}} = \frac{W^2 - 1}{ZW - 1} \quad (\text{A-7b})$$

where $Z = (\gamma + 1)/(\gamma - 1)$. In Eq. (A-7b), it is assumed that $T_w = T_\infty$. The shock Mach number M_s is related to W and Z by $M_s^2 = W(Z - 1)/(Z - W)$. Equations (A-7a) and (A-7b), combined with the tabulated results in References 11 and 12, yield the values of $I_{\infty, o}$ and G_o in Table A-1.

The constant μ solutions in References 11 and 12 have been correlated in Reference 12 by interpolation formulas. The equations

$$(f - \eta)_{\infty, o} = 1.135(W - 1)/\sqrt{1 + 1.022W} \quad (\text{A-8a})$$

$$f''(0) = -0.489(W - 1)\sqrt{1 + 1.665W} \quad (\text{A-8b})$$

correlate the numerical results in References 11 and 12 to within 1 percent.

It is also of interest to find an approximate analytic expression for $I_{\infty, o}/(f - \eta)_{\infty, o}$. This can be readily done for $\sigma = 1$ by using Eqs. (A-5) through (A-8). We find

$$\frac{I_{\infty, o}}{(f - \eta)_{\infty, o}} = [1 + 0.431\sqrt{(1 + 1.665W)(1 + 1.022W)}]/(ZW - 1) \quad (\text{A-9a})$$

$$= \frac{0.562W}{ZW - 1} \left[1 + \frac{2.57}{W} \right] [1 + 0(1/W^2)] \quad (\text{A-9b})$$

Table A-1. Parameters Defining Boundary Layer Behind Shock Moving With Uniform Velocity, Assuming an Ideal Gas and $\mu = \text{Constant}$

W	$(f - \eta)_{\infty,0}$	$f''_0(0)$	$r_0(0)$	$\sigma = 0.72$						$\sigma = 1.0$										
				$\gamma = 7/5$		$\gamma = 5/3$		$I_{s,0}$	$I_{r,0}$	$I_{s,0}$	$\gamma = 7/5$		$\gamma = 5/3$		$I_{\infty,0}$	G_0	$\gamma = 7/5$		$\gamma = 5/3$	
				$I_{\infty,0}$	G_0	$I_{\infty,0}$	G_0				$I_{\infty,0}$	G_0	$I_{\infty,0}$	G_0			$I_{\infty,0}$	G_0	$I_{\infty,0}$	G_0
1.100	0.0778	-0.08228	0.8873	1.105	0.9184	0.03392	0.1117	0.0559	0.1337	0.7780	1.108	0.0286	0.1064	0.04708	0.1249					
1.221	0.1668	-0.1883	0.8895	1.078	0.8942	0.06719	0.2340	0.1094	0.2762	0.7548	1.066	0.05616	0.2230	0.09147	0.2583					
1.500	0.3549	-0.4578	0.8937	1.025	0.8455	0.1237	0.4786	0.1979	0.5528	0.7098	1.008	0.1016	0.4565	0.1625	0.5174					
2.000	0.6466	-1.019	0.8997	0.9482	0.7767	0.1892	0.8358	0.2972	0.9438	0.6466	0.9207	0.1514	0.7980	0.2380	0.8846					
2.500	0.8977	-1.669	0.9041	0.8879	0.7231	0.2335	1.131	0.3632	1.261	0.5985	0.8542	0.1833	1.081	0.2852	1.183					
3.000	1.120	-2.397	-	-	-	-	-	-	-	0.5599	0.8003	0.2069	1.327	0.3198	1.440					
3.492	1.137	-3.184	0.9104	0.7976	0.6450	0.2964	1.614	0.4560	1.773	0.5287	0.7568	0.2256	1.543	0.3471	1.665					
4.000	1.504	-4.062	0.9129	0.7615	0.6139	0.3215	1.826	0.4930	1.997	0.5013	0.7184	0.2419	1.746	0.3709	1.875					
5.000	1.833	-5.973	-	-	-	-	-	-	-	0.4583	0.6579	0.2692	2.102	-	-					
6.000	2.124	-8.101	0.9195	0.6572	0.5255	0.3999	2.524	-	-	0.4249	0.6107	0.2922	2.417	-	-					

NOTE: Table based on data of References 11 and 12 (for $W = 1.5, 2, 3, 4, 5, 6$) and on unpublished data (for $W = 1.1, 1.221, 2.5, 3.492$).

For strong shocks, Z can be replaced by W in Eq. (A-9b).

BOUNDARY LAYER THEORY FOR LOCAL SIMILARITY SOLUTION

The boundary layer theory for use in the local similarity theory presented in the body of the report will now be outlined. For simplicity, it is assumed that $\sigma = 1$. The free stream is uniform, with a velocity u_e , and the wall has a velocity u_w (Fig. 4). The variable $V = u_e/u_{e,0}$ is introduced. As before, $W = u_w/u_{e,0}$.

Expressions for $(f - \eta)_\infty$ and $f''(0)$ are found by replacing W by W/V in Eqs. (A-8). The result is

$$(f - \eta)_\infty = 1.135 \left(\frac{W}{V} - 1 \right) \sqrt{1 + 1.022 \frac{W}{V}} \quad (\text{A-10a})$$

$$f''(0) = -0.489 \left(\frac{W}{V} - 1 \right) \sqrt{1 + 1.665 \frac{W}{V}} \quad (\text{A-10b})$$

which is valid for all σ . For $\sigma = 1$, Eq. (A-5) becomes (since $r(0) = 1$)

$$I_\infty = \frac{\gamma - 1}{2} M_e^2 \left(\frac{W}{V} - 1 \right)^2 (I_s - I_r) + \left(1 - \frac{T_w}{T_e} \right) I_s \quad (\text{A-11})$$

where

$$I_r = \frac{\left(2 \frac{W}{V} - 1 \right) (f - \eta)_\infty + f''(0)}{\left(\frac{W}{V} - 1 \right)^2} \quad I_s = \frac{(f - \eta)_\infty}{\left(\frac{W}{V} - 1 \right)}$$

But $M_e = u_e/a_e = M_{e,0} \sqrt{T_{e,0}/T_e}$ and $T_w/T_e = (T_w/T_{e,0})(T_{e,0}/T_e)$. Also, the flow in the free stream is isentropic so that $p_e/p_{e,0} = (\rho_e/\rho_{e,0})^\gamma$ and $T_e/T_{e,0} = (\rho_e/\rho_{e,0})^{\gamma-1}$. From Eqs. (A-7), (A-10), and (A-11), it can then

be shown that

$$\frac{I_{\infty}}{(f - \eta)_{\infty}} = \frac{V}{ZW - 1} \frac{WV - 1}{W - V} \frac{T_{e,o}}{T_e} \left[1 + 0.431 \frac{W - V}{WV - 1} \sqrt{(V + 1.665W)(V + 1.022W)} + \frac{ZW - 1}{WV - 1} \left(\frac{T_e}{T_{e,o}} - 1 \right) \right] \quad (\text{A-12})$$

It also follows that

$$\begin{aligned} H_e &\equiv \sqrt{V p_e / p_{e,o}} [(f - \eta)_{\infty} + I_{\infty}] \\ &= \frac{1.135W}{\sqrt{V + 1.022W}} \left(\frac{p_e}{p_{e,o}} \right)^{y/2} \left\{ 1 + \frac{V}{ZW - 1} \left(\frac{p_{e,o}}{p_e} \right)^{y-1} \left[V - Z + 0.431 \frac{W - V}{W} \sqrt{V + 1.665W} \sqrt{V + 1.022W} \right] \right\} \end{aligned} \quad (\text{A-13})$$

To integrate Eq. (16), it is necessary to express H_e as a function of δ . This is done as follows. For isentropic flow

$$\frac{p_e u_e}{(p_e u_e)_o} = \frac{M_e}{M_{e,o}} \left[\frac{Z - 1 + M_{e,o}^2}{Z - 1 + M_e^2} \right]^{Z/2}$$

which, with Eq. (8), gives

$$M_e = (1 - \delta) M_{e,o} \left[\frac{Z - 1 + M_{e,o}^2}{Z - 1 + M_e^2} \right]^{Z/2} \quad (\text{A-14})$$

which can be solved by iteration to find M_e as a function of $\bar{\delta}$. Also, for isentropic flow

$$\frac{\rho_e}{\rho_{e,o}} = \left[\frac{Z - 1 + M_{e,o}^2}{Z - 1 + M_e^2} \right]^{(Z-1)/2} \quad (\text{A-15})$$

Finally

$$V = \frac{\rho_e u_e}{(\rho_e u_e)_o} \frac{\rho_{e,o}}{\rho_e} = (1 - \bar{\delta}) \frac{\rho_{e,o}}{\rho_e} \quad (\text{A-16})$$

Equations (A-13) through (A-16) permit H_e to be found as a function of $\bar{\delta}$ and permit the integration of Eq. (16).

REFERENCES

1. I. I. Glass and G. N. Patterson, "A Theoretical and Experimental Study of Shock-Tube Flows," J. Aeronaut. Sci. 22 (2), 73-100, (1955).
2. C. duP. Donaldson and R. D. Sullivan, "The Effect of Wall Friction on the Strength of Shock Waves in Tubes and Hydraulic Jumps in Channels," NACA TN 1942, (1949).
3. R. N. Hollyer, Jr., A Study of Attenuation in the Shock Tube. Eng. Res. Inst., Univ. Michigan, July 1, 1953. (U. S. Navy Dept., Office Naval Res. Contract No. N6-ONR-232-TO IV, Proj. M720-4.)
4. R. L. Trimpi and N. B. Cohen, "A Theory for Predicting the Flow of Real Gases in Shock Tubes with Experimental Verification," NACA TN 3375, (1955).
5. H. Mirels, "Attenuation in a Shock Tube Due to Unsteady-Boundary-Layer Action," NACA Report 1333, (1957). [Supersedes NACA TN 3278]
6. H. Mirels and W. H. Braun, "Nonuniformities in Shock-Tube Flow Due to Unsteady-Boundary-Layer Action," NACA TN 4021, (1957).
7. R. E. Duff, "Shock-Tube Performance at Low Initial Pressure," Phys. Fluids 2 (2), 207-216 (1959).
8. A. Roshko, "On Flow Duration in Low-Pressure Shock Tubes," Phys. Fluids 3, 835 (1960).
9. G. F. Anderson, "Shock-Tube Testing Time," J. Aero/Space Sci. 26, 184 (1959).
10. W. J. Hooker, "Testing Time and Contact Zone Phenomena in Shock Tube Flows," Phys. Fluids 4, 1451 (1961).
11. H. Mirels, "Laminar Boundary Layer Behind a Shock Advancing into Stationary Fluid," NACA TN 3401, (1955).
12. H. Mirels, "Boundary Layer Behind Shock or Thin Expansion Wave Moving into Stationary Fluid," NACA TN 3712, (1956).
13. H. Mirels, "Laminar Boundary Layer Behind a Strong Shock Moving into Air," NASA TN D-291, (1961).
14. J. C. Camm and P. H. Rose, "Electric Shock Tube for High Velocity Simulation." AVCO-Everett Research Report 136, Avco Corp., Everett, Mass. (July 1962).

15. V. A. Sandborn, "Measurements of Flow Duration in a Low-Pressure Shock Tube," NASA TN D-1218, (1962).
16. H. Mirels, "The Wall Boundary Layer Behind a Moving Shock Wave," Boundary Layer Research, Proc. International Union of Theoretical and Applied Mechanics, H. Gortler, ed. (Springer Verlag, Berlin, 1958). pp. 283-293.
17. R. A. Hartunian, A. L. Russo, and P. V. Marrone, Boundary-Layer Transition and Heat Transfer in Shock Tubes. J. Aerospace Sci. 27, (8) (1960).
18. S. Ostrach and P. R. Thornton, "Stability of Compressible Boundary Layers Induced by a Moving Wave," J. Aerospace Sci. 29 (3) (1962).

UNCLASSIFIED

Aerospace Corporation, El Segundo, California.
TEST TIME IN LOW PRESSURE SHOCK TUBES,
prepared by Harold Mirels. 27 December 1962.
[78] p. incl. illus.
(Report TDR-169(3230-12)TN-5; SSD-TDR-62-204)
(Contract AF 04(695)-169) Unclassified report

The reduction of test time in low pressure shock tubes, due to a laminar wall boundary layer, has been analytically investigated. In previous studies by Roshko and Hooker the flow was considered in a contact surface fixed co-ordinate system. In the present study it was assumed that the shock moves with uniform velocity, and the flow was investigated in a shock fixed co-ordinate system. Unlike the previous studies, the variation of free stream conditions between the shock and contact surface was taken into account. It was found that β , a parameter defined by Roshko, is considerably larger than the estimates made by Roshko and

(over)

UNCLASSIFIED

UNCLASSIFIED

Aerospace Corporation, El Segundo, California.
TEST TIME IN LOW PRESSURE SHOCK TUBES,
prepared by Harold Mirels. 27 December 1962.
[78] p. incl. illus.
(Report TDR-169(3230-12)TN-5; SSD-TDR-62-204)
(Contract AF 04(695)-169) Unclassified report

The reduction of test time in low pressure shock tubes, due to a laminar wall boundary layer, has been analytically investigated. In previous studies by Roshko and Hooker the flow was considered in a contact surface fixed co-ordinate system. In the present study it was assumed that the shock moves with uniform velocity, and the flow was investigated in a shock fixed co-ordinate system. Unlike the previous studies, the variation of free stream conditions between the shock and contact surface was taken into account. It was found that β , a parameter defined by Roshko, is considerably larger than the estimates made by Roshko and

(over)

UNCLASSIFIED

UNCLASSIFIED

Aerospace Corporation, El Segundo, California.
TEST TIME IN LOW PRESSURE SHOCK TUBES,
prepared by Harold Mirels. 27 December 1962.
[78] p. incl. illus.
(Report TDR-169(3230-12)TN-5; SSD-TDR-62-204)
(Contract AF 04(695)-169) Unclassified report

The reduction of test time in low pressure shock tubes, due to a laminar wall boundary layer, has been analytically investigated. In previous studies by Roshko and Hooker the flow was considered in a contact surface fixed co-ordinate system. In the present study it was assumed that the shock moves with uniform velocity, and the flow was investigated in a shock fixed co-ordinate system. Unlike the previous studies, the variation of free stream conditions between the shock and contact surface was taken into account. It was found that β , a parameter defined by Roshko, is considerably larger than the estimates made by Roshko and

(over)

UNCLASSIFIED

UNCLASSIFIED

Aerospace Corporation, El Segundo, California.
TEST TIME IN LOW PRESSURE SHOCK TUBES,
prepared by Harold Mirels. 27 December 1962.
[78] p. incl. illus.
(Report TDR-169(3230-12)TN-5; SSD-TDR-62-204)
(Contract AF 04(695)-169) Unclassified report

The reduction of test time in low pressure shock tubes, due to a laminar wall boundary layer, has been analytically investigated. In previous studies by Roshko and Hooker the flow was considered in a contact surface fixed co-ordinate system. In the present study it was assumed that the shock moves with uniform velocity, and the flow was investigated in a shock fixed co-ordinate system. Unlike the previous studies, the variation of free stream conditions between the shock and contact surface was taken into account. It was found that β , a parameter defined by Roshko, is considerably larger than the estimates made by Roshko and

(over)

UNCLASSIFIED

<p>Hooker except for very strong shocks. Since test time is proportional to β^{-2}, previous estimates of test time are too large, particularly for weak shocks. The present estimates for β appear to agree with existing experimental data to within about 10 percent for shock Mach numbers greater than 5. In other respects, the basic theory is in general agreement with the previous results of Roshko.</p>	<p>UNCLASSIFIED</p>
<p>Hooker: except for very strong shocks. Since test time is proportional to β^{-2}, previous estimates of test time are too large, particularly for weak shocks. The present estimates for β appear to agree with existing experimental data to within about 10 percent for shock Mach numbers greater than 5. In other respects, the basic theory is in general agreement with the previous results of Roshko.</p>	<p>UNCLASSIFIED</p>

<p>Hooker except for very strong shocks. Since test time is proportional to β^{-2}, previous estimates of test time are too large, particularly for weak shocks. The present estimates for β appear to agree with existing experimental data to within about 10 percent for shock Mach numbers greater than 5. In other respects, the basic theory is in general agreement with the previous results of Roshko.</p>	<p>UNCLASSIFIED</p>
<p>Hooker except for very strong shocks. Since test time is proportional to β^{-2}, previous estimates of test time are too large, particularly for weak shocks. The present estimates for β appear to agree with existing experimental data to within about 10 percent for shock Mach numbers greater than 5. In other respects, the basic theory is in general agreement with the previous results of Roshko.</p>	<p>UNCLASSIFIED</p>